Cooperative Transformations of Small Molecules at a Dinuclear Nickel(II) Site

Franc Meyer,* Elisabeth Kaifer, Peter Kircher, Katja Heinze, and Hans Pritzkow[a]

Abstract: Using the possibility of tuning the metal–metal distance in pyrazolate-based bimetallic complexes by the length of the chelating side arms attached to the heterocycle, we have synthesized related dinickel(II) complexes in which either a hydroxide (**1**) or a H_3O_2 unit (**2**) spans the two metal centers within the bimetallic pocket. Complex **1** exhibits strong antiferromagnetic coupling mediated by the bridging hydroxide unit ($J = -56.9$ cm^{-1}), while **2** shows Curie–Weiss behavior over a wide temperature range. The H_3O_2 unit in **2** acts like the resting form of an active metal-bound hydroxide and allows the study of cooperative transformations of small molecules at a dinickel(II) site relevant to the active site of the metalloenzyme urease. Firstly, it mediates the hydration of various nitriles to give the respective μ-amidato-N,O-bridged complexes **3a**–**c**. Reaction of **2** with urea affords complex **5** with an N,O-bridging deprotonated urea, which when heated releases ammonia to yield the cyanato-bridged dinickel(II) compound **4**. This product is also obtained when **2** is treated with dimethylcyanamide. Unactivated amides dimethylformamide (DMF) and dimethylamide (DMA) are hydrolyzed by **2** only sluggishly, while the stoichiometric hydrolysis of esters such as ethyl acetate and ethyl propionate runs more cleanly to afford the carboxylato-bridged bimetallic complexes **10b** and **c**. Likewise, hydrolytic cleavage occurs with γ-butyrolactone to give complex **10d**. We propose that these reactions proceed by cooperative action of the two metal ions within the bimetallic pocket of the dinickel(II) core. Possible alternatives are addressed by investigation of analogous mononuclear nickel(II) complexes **8a** and **b** in conjunction with a corresponding dimeric compound **9** and by the reaction of **2** with an excess of acetate to yield the dinickel(II) complex **11**, in which a formerly chelating side arm has been driven out of the coordination sphere. Complexes **1**·$(BPh_4)_2$, **2**·$(BPh_4)_2$, **3c**·$(ClO_4)_2$, **4**·$(BPh_4)_2$, **8b**·$(ClO_4)_2$, **9**·$(ClO_4)_2$, **10d**·$(ClO_4)_2$, and **11**·(ClO_4) have been characterized structurally by X-ray crystallography.

Keywords: bioinorganic chemistry · cooperative effects · dinuclear complexes · enzyme mimetics · nickel

Introduction

Numerous enzymes that catalyze the hydrolysis of biologically relevant substrates such as phosphate esters or amides (peptides or urea) are known to employ two divalent metal ions in close proximity within their active site.[1] Although various specific mechanisms are most probably involved for the individual catalytic processes, a dominant feature is believed to be that one metal center acts as a Lewis acid to increase the pK_A of bound water and thus delivers the hydroxide nucleophile to the substrate, which itself may be bound to the adjacent second metal ion.[2] The prominent nickel-containing enzyme urease that degrades urea to ammonia and carbamate (and finally CO_2) is assumed to follow these lines,[3] as has been corroborated by a series of crystallographic and functional studies.[4–6] Thus, the widely accepted mechanism for urease activity suggests that urea is activated by coordination to one nickel(II) ion in conjunction with extensive hydrogen bonding within the active site pocket of the protein and is subsequently attacked by a nucleophilic hydroxide bound to the opposite nickel(II) center; the resulting carbamate then decomposes further to yield carbonic acid and another molecule of ammonia.[3, 6] It should be noted, however, that more recent structural findings of both native and inhibited urease, together with structure-based molecular modeling of the catalytic mechanism, point to the possibility of a bridging coordination mode of both urea and hydroxide at the active dinickel(II) site, which underlines that the fine details of substrate binding and enzyme activity of urease are still far from being fully clarified.[7]

In order to elucidate structural and mechanistic aspects of such dinuclear hydrolases and to mimic their hydrolytic activity, various bimetallic complexes related to active-site structures have been studied.[8, 9] On the basis of the urease mechanism outlined above, it appears desirable to design systems which contain a HO^- nucleophile bound to one metal ion and an accessible coordination site at a second, adjacent metal center. We recently described a series of pyrazolate-

[a] Dr. F. Meyer, Dr. E. Kaifer, Dr. P. Kircher, Dr. K. Heinze, Dr. H. Pritzkow
Anorganisch-Chemisches Institut der Universität Heidelberg
Im Neuenheimer Feld 270, D-69120 Heidelberg (Germany)
Fax: (+49) 6221-545707
E-mail: franc@sun0.urz.uni-heidelberg.de

  0947-6539/99/0505-1617 $ 17.50+.50/0

based dinuclear complexes in which appropriate chelating side arms attached to the heterocycle may enforce metal–metal separations large enough to prevent small monoatomic units like HO^- from spanning both metal centers, but instead favor the formation of intramolecular $H_3O_2^-$ secondary bridges.[10, 11] Extrusion of water from these moieties—a process for which experimental evidence was obtained for a FHO(H)-bridged dicobalt(II) complex of this type[10]—or its replacement by potential substrates might then create the favorable geometry that facilitates hydrolysis. In the case of some μ-oxo-diiron(III) complexes, an intramolecular secondary $H_3O_2^-$ bridge has previously been shown to promote the hydration of acetonitrile and the hydrolytic cleavage of activated phosphate esters.[12] In the context of our model studies for urease and related hydrolase metalloenzymes, and our search for cooperative substrate transformations at bimetallic sites,[10, 11, 13, 14] we report here the synthesis and characterization of a dinickel(II) complex which features an intramolecular H_3O_2 moiety. Comparison with a related HO-bridged compound and the hydrolytic transformation of nitriles, urea, unactivated amides, and esters at the bimetallic core are presented.

Results and Discussion

The ligands HL^1 and HL^2 were employed for the synthesis of dinuclear nickel(II) complexes. These ligands have previously been shown to provide two adjacent tran-type coordination compartments (tran = tris(aminoalkyl)amine) suitable for N_4X ligation of 3d transition metal ions (Scheme 1).[10, 15]

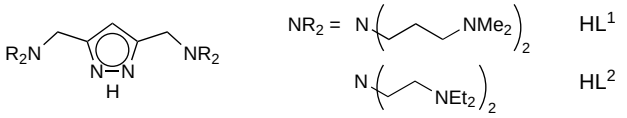

Scheme 1. Ligands HL^1 and HL^2 used in the synthesis of dinuclear nickel(II) complexes.

Treatment of these potential ligands each with two equivalents of $[Ni(H_2O)_6](ClO_4)_2$ and LiOEt afforded the dinickel(II) complexes $[L^1Ni_2(OH)](ClO_4)_2$ (**1**·$(ClO_4)_2$) and $[L^2Ni_2(O_2H_3)](ClO_4)_2$ (**2**·$(ClO_4)_2$), which were obtained in crystalline form as the respective BPh_4^- salts after anion exchange. Their molecular structures were determined by X-ray diffraction and the cations **1** and **2** are depicted in Figure 1.

As was the case for the analogous dizinc(II) species,[11] in **1** a hydroxide is found as a monoatomic bridge spanning two five-coordinate nickel atoms with a metal–metal separation of $d(Ni\cdots Ni) = 3.643$ Å. In contrast, the shorter ligand side arms of L^2 pull the two metal centers back and apart [$d(Ni\cdots Ni) = 4.452$ Å] to prevent a bridging position for the small hydroxide but induce incorporation of an additional water molecule, and thus establish a $H_3O_2^-$ moiety with a very strong[16] intramolecular hydrogen bridge [$d(O1\cdots O2) = 2.433$ Å]. The terminal H atoms were located in weak hydrogen bonds to two acetone solvent molecules incorporated in the crystal lattice [$d(O1\cdots O3) = 2.933$ Å; $d(O2\cdots O4) = 2.928$ Å].

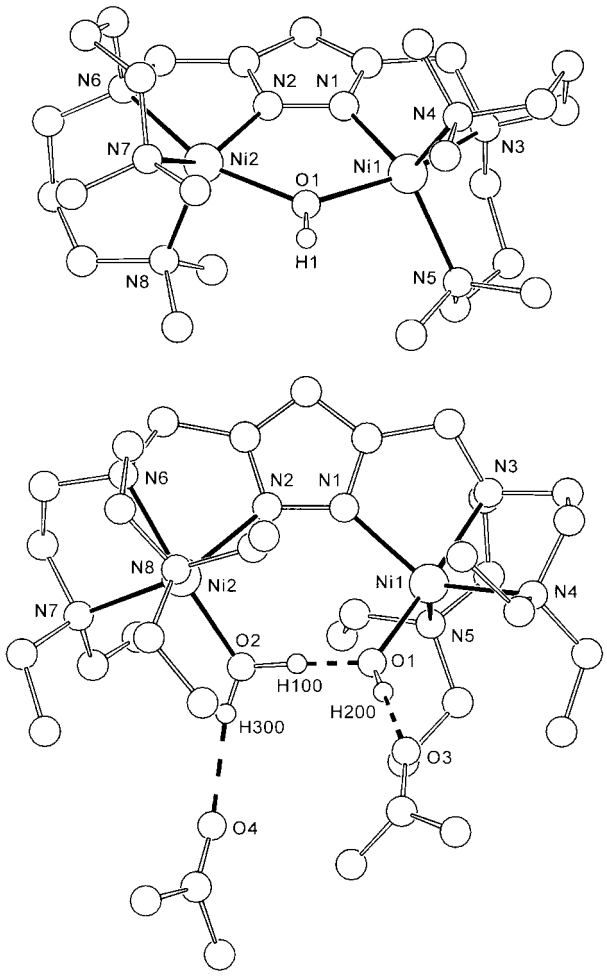

Figure 1. Molecular structure of cation **1** (top) and **2** (bottom). In the interests of clarity most of the hydrogen atoms have been omitted. Selected interatomic distances [Å] and bond angles [°] for **1**: Ni1–O1 2.065(2), Ni1–N1 1.947(2), Ni1–N3 2.239(2), Ni1–N4 2.061(2), Ni1–N5 2.125(2), Ni2–O1 2.074(2), Ni2–N2 1.937(2), Ni2–N6 2.225(2), Ni2–N7 2.116(2), Ni2–N8 2.080(2), N1–N2 1.351(3), Ni1 ··· Ni2 3.643; Ni1-O1-Ni2 123.28(9), O1-Ni1-N3 156.54(8), N1-Ni1-N5 145.1(1), O1-Ni2-N6 158.09(8), N2-Ni2-N7 142.5(1). For **2**: Ni1–O1 1.947(2), Ni1–N1 2.038(2), Ni1–N3 2.111(3), Ni1–N4 2.222(3), Ni1–N5 2.169(3), Ni2–O2 1.966(2), Ni2–N2 2.057(2), Ni2–N6 2.107(3), Ni2–N7 2.199(3), Ni2–N8 2.134(3), N1–N2 1.369(3), Ni1 ··· Ni2 4.452, O1 ··· O2 2.433, O1 ··· O3 2.933, O2 ··· O4 2.928; O1-Ni1-N3 175.3(2), N1-Ni1-N4 134.0(2), O1-Ni2-N6 169.8(2), N2-Ni2-N7 133.9(2).

The nickel ions in both complexes are five-coordinate; however, they adopt a different geometry in the continuum between a perfect trigonal-bipyramidal (TB-5) and a square-pyramidal (SPY-5) structure. By means of the angular structural parameter $\tau = (\beta - \alpha)/60$ introduced by Addison et al.,[17] where α and β represent two basal angles with $\beta > \alpha$, the degree of trigonality in **1** and **2** can be evaluated (a perfect TB-5 structure is associated with $\tau = 1$, while $\tau = 0$ is expected for ideal SPY-5 geometry). While the coordination sphere around the nickel ions in **2** ($\tau = 0.60$ and 0.69) exhibits marked TB-5 character with the branching nitrogen donors N3 and N6 and the oxygen atoms of the H_3O_2 unit in the axial positions, the geometry in **1** is expressed by a square pyramid ($\tau = 0.19$ and 0.26) due to the small size of the secondary HO bridge, which forces the angles N3-Ni1-O1

0947-6539/99/0505-1618 $ 17.50+.50/0 *Chem. Eur. J.* **1999**, *5*, No. 5

[156.54(8)°] and N6-Ni2-O1 [158.09(8)°] to be significantly smaller than 180°.

Basic properties of the dinickel complexes 1 and 2: The different secondary bridges in **1** and **2** also manifest themselves in the different magnetic properties of these two complexes. Magnetic susceptibility data at 10 kG were recorded over the temperature range 10.4–280 K [**1**·$(BPh_4)_2$] and 5.7–250 K [**2**·$(BPh_4)_2(acetone)_2$], and are shown in Figure 2.

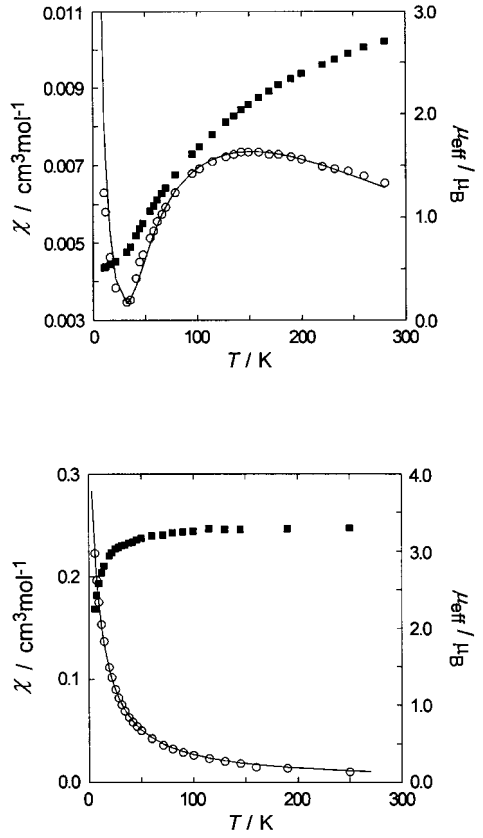

Figure 2. Temperature dependence of the molar magnetic susceptibility (○) and magnetic moment (■) per nickel atom for **1**·$(BPh_4)_2$ (top) and **2**·$(BPh_4)_2$ (bottom). The solid line represents the calculated fit (see text).

While the data for **2**·$(BPh_4)_2(acetone)_2$ are in accordance with Curie–Weiss behavior over a wide temperature range ($C = 2.93$; $\theta = -7.33$) and thus indicate no significant coupling between the two paramagnetic centers, the susceptibility curve for **1**·$(BPh_4)_2$ exhibits a broad maximum at around 150 K with the magnetic moment per nickel ion gradually decreasing from 2.71 μ_B at 280 K to 0.51 μ_B at 10.4 K. This behavior is indicative of strong antiferromagnetic exchange between the two nickel(II) centers, mediated predominantly by the bridging hydroxide.[18] An increase of the susceptibility values at very low temperatures is probably due to the presence of small amounts of uncoupled paramagnetic impurity. When the experimental data is fit to the theoretical expression for the isotropic spin Hamiltonian $\boldsymbol{H} = -2J \cdot \boldsymbol{S}_1 \cdot \boldsymbol{S}_2$ (with $S_1 = S_2 = 1$) including a molar fraction p of uncoupled paramagnetic impurity, Equation (1) yields $J = -56.9\ cm^{-1}$, $g = 2.42$ and $p = 2.9\%$.[18–20]

$$\chi = \chi_{dim}(1-p) + 2\chi_{mono}p + 2N_\alpha \quad (1)$$

In principle, powder measurements are not ideally suited for a thorough analysis of $S = 1$ dinuclear systems; however, the intradimer exchange term J often proves to be the dominant term in the spin Hamiltonian,[21] and accordingly neglect of both a zero-field splitting parameter D and interdimer interactions $z'J'$ results in a fit of reasonable quality in the present case (Figure 2). The value of $J = -56.9\ cm^{-1}$ in **1**·$(BPh_4)_2$ lies in the upper range of the exchange interactions reported previously for OH^- or pyrazolate-bridged nickel(II) dimers.[13, 21, 22] Magnetostructural relationships for dinuclear Ni^{II} systems are not yet as elaborated as the detailed correlations noted in Cu^{II}/Cu^{II} chemistry,[18, 23] but only recently a linear dependence of the antiferromagnetic exchange coupling constant on Ni-O-Ni bridge angles as well as on the intramolecular Ni···Ni distances in a series of doubly phenoxy-bridged dinickel(II) complexes emerged.[24] From those studies it was concluded that the antiferromagnetic exchange interaction increases with an increase of the bridge angle Ni-O-Ni involved in the superexchange pathway and that it becomes substantially augmented on going from six-coordinate species to five-coordinate square pyramidal species. Our observation of a rather large coupling constant for the five-coordinate nickel(II) centers in **1**·$(BPh_4)_2$, which shows a large Ni-O-Ni angle of 123.28(9)° at the bridging OH group, is thus in good agreement with the reported trend. However, we recently reported a related μ-hydroxo-μ-pyrazolatodinickel(II) complex[13] that also features five-coordinate metal centers with a nearly identical bridge angle Ni-O-Ni [123.4(2)°] and an even shorter Ni···Ni distance [3.476 versus 3.643 Å in **1**] but which nevertheless exhibits a somewhat smaller exchange coupling constant of $J = -46.7\ cm^{-1}$. Obviously the distinct coordination geometry of the individual nickel(II) ions, such as the degree of trigonality ($\tau = 0.02/0.20$[13] versus 0.19/0.26 in **1**), must be taken into account for a comprehensive understanding of the magnetic properties of such nickel(II) dimers.

Acetonitrile solutions of both complexes, **1**·$(BPh_4)_2$ and **2**·$(ClO_4)_2$, were studied by cyclic voltammetry in the potential range −1.8 to +1.5 V versus SCE (Table 1). All redox chemistry, which we assume to be metal-centered, is found to be electrochemically irreversible over the entire range of scan rates studied (50–1000 $mV\,s^{-1}$) with oxidation peak potentials $E_p^{ox} = +1.02$ V (**1**) and +1.34 V (**2**) and reductions at $E_p^{red} \approx -1.7$ V (**1**; broad featureless wave) and −1.31 V (**2**). It thus transpires that the longer and more flexible ligand side arms in **1** are comparatively more favorable to support an oxidized species than the smaller chelate rings enforced by the shorter side arms in **2**, in agreement with previous findings.[25]

Table 1. Cyclic voltammetry of the complexes in MeCN.

	E_p^{red} (ΔE at 200 $mV\,s^{-1}$)	E_p^{ox} (ΔE at 200 $mV\,s^{-1}$)
1·$(BPh_4)_2$	≈−1.7 (irrev, broad)	+1.02 (irrev)
2·$(ClO_4)_2$	−1.31 (irrev)	+1.34 (irrev)
3a·$(ClO_4)_2$	−1.37 (irrev)	≈+1.5 (irrev, broad)
3c·$(ClO_4)_2$	−1.30 (172, quasirev)	+1.38 (irrev)
4·$(BPh_4)_2$	−1.07 (140, quasirev)	+0.90 (irrev)
5·$(ClO_4)_2$	−1.34 (irrev)	≈+1.4 (irrev, broad)
10c·$(ClO_4)_2$	−1.22 (142, quasirev)	+1.67 (irrev)

Transformation of nitriles and urea at 2: The H_3O_2 entity in **2** may be viewed as a hydrated, that is, resting form of a Ni-OH unit in close proximity to a second Lewis-acidic nickel center. For a related FHO(H)-bridged dicobalt(II) complex, evidence could be obtained for the possibility of reversible extrusion of the incorporated water molecule,[10] and this is further corroborated by the mass spectrometric findings in the present case. The FAB mass spectrum of $\mathbf{2}\cdot(ClO_4)_2$ reveals dominant signals for both $[L^2Ni_2(OH)(ClO_4)]^+$ and $[L^2Ni(O_2H_3)(ClO_4)]^+$ (with the intensity of the latter increasing at the expense of the former during higher scan numbers), which suggests partial extrusion of water from **2** under the conditions of the MS experiment.

In order to model hydrolytic reactions at dinuclear nickel(II) centers, we first tested the ability of **2** to hydrate nitriles to the corresponding amides. Heating $\mathbf{2}\cdot(ClO_4)_2$ in acetonitrile, acrylonitrile, or benzonitrile to 75 °C does not cause any significant changes to the solution UV spectra (see Table 2),

Table 2. UV/Vis data of the complexes; λ [nm] (ε [$M^{-1}cm^{-1}$]).

$\mathbf{1}\cdot(BPh_4)_2$[a]	390 (270), 621 (100)
$\mathbf{2}\cdot(BPh_4)_2$[b]	405 (290), 475 (sh), 653 (65)
$\mathbf{3a}\cdot(BPh_4)_2$[a]	410 (310), 649(95)
$\mathbf{3a}\cdot(ClO_4)_2$[b]	408 (265), 470 (sh), 650 (75)
$\mathbf{3b}\cdot(ClO_4)_2$[b]	407 (195), 475 (sh), 650 (60)
$\mathbf{3c}\cdot(ClO_4)_2$ [b]	407 (225), 475 (sh), 653 (65)
$\mathbf{4}\cdot(BPh_4)_2$[b]	413 (275), 667 (92)
$\mathbf{5}\cdot(ClO_4)_2$[b]	408 (300), 477 (sh), 649 (70)
$\mathbf{8a}\cdot(ClO_4)_2$[a]	368 (sh), 575 (15), 1040 (20)
$\mathbf{8b}\cdot(ClO_4)_2$[a]	367 (sh), 575 (15), 1040 (20)
$\mathbf{9}\cdot(ClO_4)_2$[a]	403 (315), 630(90), 777 (40)
$\mathbf{10a}\cdot(BPh_4)_2$[b]	412 (260), 655 (95)
$\mathbf{10b}\cdot(BPh_4)_2$[b]	408 (290), 652 (95)
$\mathbf{10b}\cdot(ClO_4)_2$[b]	414 (245), 660 (85)
$\mathbf{10c}\cdot(ClO_4)_2$[b]	411 (250), 656 (80)
$\mathbf{10d}\cdot(BPh_4)_2$[b]	414 (350), 657 (120)

[a] in MeCN. [b] In acetone.

but FAB mass spectra of the isolated materials display dominant peaks that are in accordance with compositions $[L^2Ni_2\{NH(O)CR\}(ClO_4)]^+$ and $[L^2Ni_2\{NH(O)CR\}]^+$ [R = CH_3 (**3a**), C_2H_3 (**3b**), Ph (**3c**)] with the expected isotopic distribution pattern, which indicates conversion of **2** to the respective μ-(amidato-N,O) bridged complexes (**3a**–**c**; Scheme 2).

This is further confirmed by the appearance of characteristic IR bands at 3300–3365 cm^{-1} [assigned to ν(N–H) of the amidato bridge] and in the 1450–1630 cm^{-1} region [ν(NCO)]. No products from attack at the alkene moiety are observed for **3b**. Complex **3a** can be prepared independently by treatment of **2** with acetamide. This reaction is similar to the deprotonation of urea by **2** (vide infra) and expresses the ability of **2** to act as a base. Final structural proof for the identity of **3a**–**c** comes from an X-ray crystallographic analysis of $\mathbf{3c}\cdot(ClO_4)_2$, the result of which is shown in Figure 3.

The molecular structure of the cation reveals the presence of the amidato unit which stems from the respective nitrile within the coordination pocket of the bimetallic framework. Both nickel ions have remained five-coordinate with geometries intermediate between TB-5 and SPY-5 (τ around

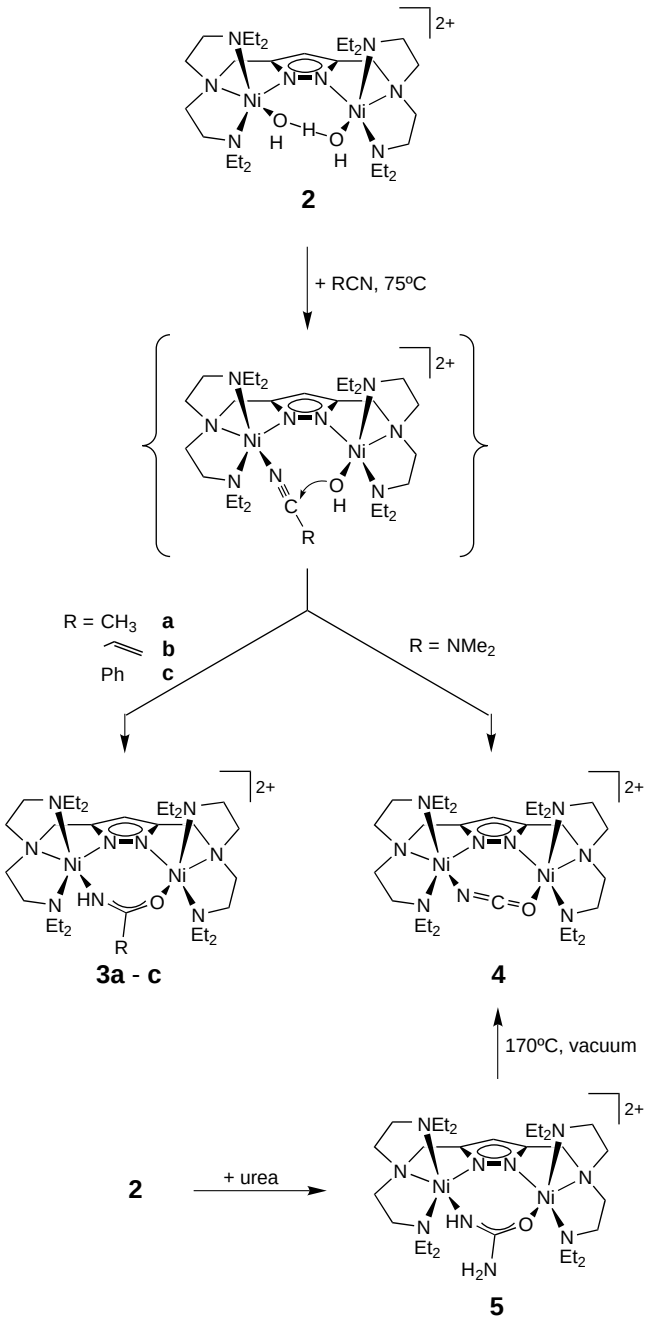

Scheme 2. Synthesis of **3a**–**c**, **4**, and **5**.

0.50) while the Ni1···Ni2 distance [4.285 Å] is somewhat shortened compared to the starting complex **2**. The C30–O1 and C30–N9 bond lengths of the benzamidate are 1.275(5) and 1.294(5) Å, and the torsion angle between the plane of the phenyl ring and those defined by the amidato unit (O1-C30-N9) amounts to 33.9°. These values are well within the range expected for the anionic ligand when compared to those of the free neutral benzamide [1.24 Å, 1.31 Å, 26°].[26]

We assume that hydration of nitriles by **2** proceeds as outlined in the upper part of Scheme 2. Replacement of an exchangeable water molecule of the H_3O_2 unit by an N-coordinated nitrile substrate places the carbon atom of the latter in a well-situated position for nucleophilic attack by

0947-6539/99/0505-1620 $ 17.50+.50/0 *Chem. Eur. J.* **1999**, *5*, No. 5

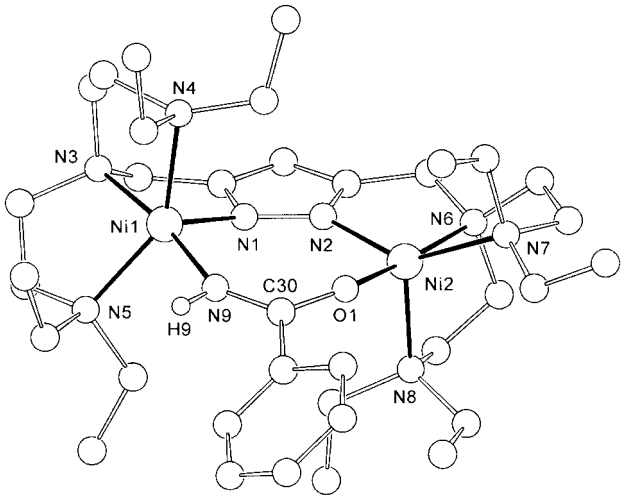

Figure 3. Molecular structure of cation **3c**. In the interests of clarity most of the hydrogen atoms have been omitted. Selected interatomic distances [Å] and bond angles [°]: Ni1–N9 2.001(3), Ni1–N1 1.993(3), Ni1–N3 2.131(4), Ni1–N4 2.132(4), Ni1–N5 2.05(2), Ni2–O1 1.985(3), Ni2–N2 2.021(3), Ni2–N6 2.119(3), Ni2–N7 2.199(3), Ni2–N8 2.094(3), N1–N2 1.388(5), Ni1 ··· Ni2 4.285; N3-Ni1-N9 171.9(2), N4-Ni1-N5 142.1(4), O1-Ni2-N6 173.5(2), N2-Ni2-N7 143.8(2), N9-C30-O1 125.9(4).

the hydroxide group bound to the second, adjacent nickel ion. A final proton shift then establishes the very stable μ-(amidato-N,O) bridges in **3a–c**. Similar reaction mechanisms have previously been suggested for nitrile hydration at dinuclear iron(III),[12] cobalt(III),[27] copper(II)[28] palladium(II)[29] and rhenium(III)[30] sites. It should be pointed out that no such reaction was observed for **1** under identical reaction conditions, which underlines the deactivation of the metal-bound hydroxide by its tight fixation in a bridging position between the two metal ions.

When the amino-substituted nitrile dimethylcyanamide was employed, the reaction took a different course and the cyanato-bridged complex **4** was isolated in 42% yield (Scheme 2). In view of the formation of **3a–c**, hydration of the nitrile function of the cyanamide appears to be a first step, generating a N′,O-bridging deprotonated *N,N*-dimethylurea which spans the two nickel ions and subsequently loses dimethylamine to yield **4**. The reaction of **2** with parent cyanamide proceeds differently to yield a 2-cyanoguanidine moiety that remains coordinated to the bimetallic core.[31] Nevertheless, a bridging coordination mode of deprotonated parent urea at a dinickel(II) site that formed upon treatment of **2** with either urea or *N,N*-bis(trimethylsilyl)urea (Scheme 2) was recently observed in **5** and confirmed crystallographically for the first time.[14] However, only starting material was recovered when a solution of **2** in acetone was treated with *N,N*-dimethylurea; this is probably due to the lower acidity of N-methylated urea compared to the parent urea. In contrast to the presumed intermediate during the reaction of dimethylcyanamide with **2**, the molecular arrangement in **5** exhibits considerable stability.[14] We believe this to reflect the greater ability of a pendant NMe_2 to act as a leaving group, which finally causes the more facile evolution of dimethylamine after initial hydration of N-coordinated dimethylcyanamide by **2**. In order to assess suitable conditions for evolution of ammonia from $\mathbf{5}\cdot(ClO_4)_2$ to analogously form $\mathbf{4}\cdot(ClO_4)_2$, a differential scanning calorimetry (DSC) experiment was performed (Figure 4). It revealed a slightly endothermic process in the temperature range 98–120 °C (peaking

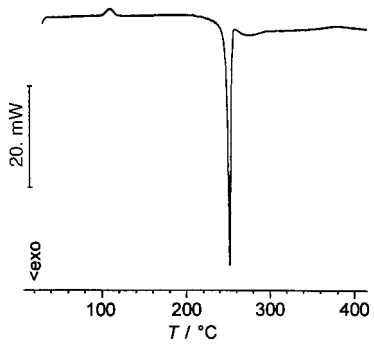

Figure 4. DSC analysis of $\mathbf{5}\cdot(ClO_4)_2$ (9.2 mg; heating rate 5 °C min^{-1}).

at 109 °C; the broad peak is detectable only at sufficiently slow heating rates) in addition to the main decomposition at around 255 °C. Mass spectrometry and IR spectroscopic data from a DSC sample that was only heated to 170 °C confirmed its conversion to $\mathbf{4}\cdot(ClO_4)_2$. These results were then applied to corresponding reactions on a preparative scale. We found that neat **5** (as the ClO_4^- or BPh_4^- salt) transforms to **4** upon heating to elevated temperatures ($\approx$170 °C; Scheme 2) under dynamic vacuum for prolonged periods, as evidenced and monitored by the gradual appearance of a characteristic IR band at 2195 cm^{-1} for the μ-1,3 cyanato moiety (asymmetric cyanate stretching vibration). Structural confirmation came from an X-ray crystallographic analysis on a single crystal of $\mathbf{4}\cdot(BPh_4)_2$ (Figure 5) that was obtained by layering an acetone

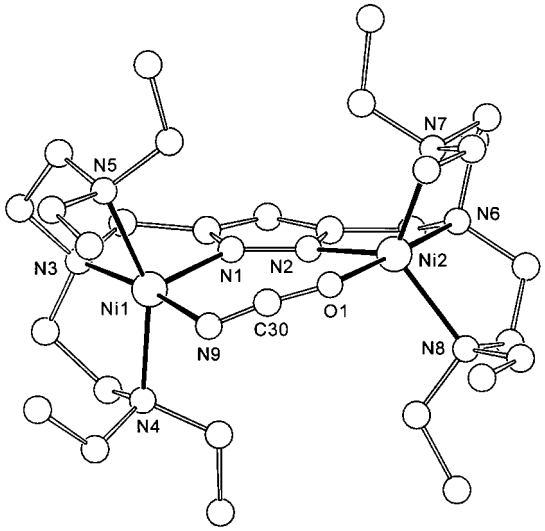

Figure 5. Molecular structure of cation **4**. In the interests of clarity the hydrogen atoms have been omitted. Selected interatomic distances [Å] and bond angles [°]: Ni1–N9 2.042(8), Ni1–N1 2.000(7), Ni1–N3 2.073(7), Ni1–N4 2.109(8), Ni1–N5 2.133(8), Ni2–O1 2.027(8), Ni2–N2 2.018(7), Ni2–N6 2.087(7), Ni2–N7 2.155(8), Ni2–N8 2.099(8), N1–N2 1.367(9), Ni1 ··· Ni2 4.383; N3-Ni1-N9 173.1(3), N4-Ni1-N5 153.9(3), O1-Ni2-N6 178.1(3), N2-Ni2-N8 119.8(3), N9-C30-O1 172(1), Ni1-N9-C30 110.6(8), Ni2-O1-C30 123.4(8).

solution of the product with light petroleum. In accordance with the IR spectroscopy data, a nearly linear cyanato bridge [N9-C30-O1 = 172(1)°] spans the two nickel centers in an end-to-end mode by the terminal atoms N9 and O1, which increases the Ni···Ni distance to 4.383 Å [d(Ni···Ni) = 4.257 Å in **5**[14]]. The two nickel ions have strongly differing coordination environments [τ = 0.32 (Ni1) and 0.97 (Ni2)] and are located 0.273 Å above (Ni2) and 0.377 Å below (Ni1) the plane defined by the pyrazolate heterocycle. With the C30 atom of the cyanate moiety situated close to this plane (distance 0.166 Å), the bond axis N9-C30-O1 intersects the plane defined by the pyrazolate by an angle of around 18°. Only three nickel(II) systems with end-to-end cyanato bridges have previously been structurally characterized,[32] and consist either of bis(cyanato) bridged dimeric units or one-dimensional nickel cyanato chains. In those cases the coordination of the cyanato bridges showed strongly asymmetric bond lengths and angles: d(Ni–O) = 2.21 – 2.34 Å and Ni-O-C = 117 – 132° versus d(Ni–N) = 2.01 – 2.08 Å and Ni-N-C = 150 – 164°,[32] while the cyanato bridge is much more symmetrical in **4**. In particular, the distances d(Ni1–N9) = 2.042(8) and d(Ni2–O1) = 2.027(8) Å are very similar (the latter being remarkably short) and the angle Ni1-N9-C30 = 110.6(8) is much smaller than in all previous cases. This particular situation in **4** appears to be caused by the rigid pyrazolate-based ligand framework, which enforces a comparatively short Ni···Ni intradimer distance (4.383 Å in **4** versus 5.38 – 6.29 Å in the previously characterized complexes[32]) and thus brings about a major contribution of the resonance form **B** at the expense of form **A** (Scheme 3).

Scheme 3. Resonance forms of the end-to-end cyanato bridge.

The elimination reaction which produces ammonia and cyanic acid from urea is known to occur in the very slow uncatalyzed decomposition of urea in aqueous solution.[33] In addition, cyanato complexes have been observed after acid-induced elimination of ammonium ion from N-coordinated urea in mononuclear rhodium(III), cobalt(III), and palladium(II) compounds.[34, 35] The present work now demonstrates a related thermal decomposition pathway for urea after fixation of the substrate in the clamp of a dinuclear nickel(II) complex.

Analogous mononuclear complexes: Although the two-metal-ion mechanism postulated for the hydration of nitriles by **2** (Scheme 2) and by some other bimetallic systems is a reasonable assumption, it should be emphasized at this point that the cooperative involvement of both metal centers during the hydration step is not directly proven. In order to address this point we prepared the related mononucleating ligand systems HL^3 and HL^4, which bear a single donor side arm only (Scheme 4).

Relatively few unsymmetric pyrazole ligands attached to polyamine moieties by the C3 atom only have been studied up

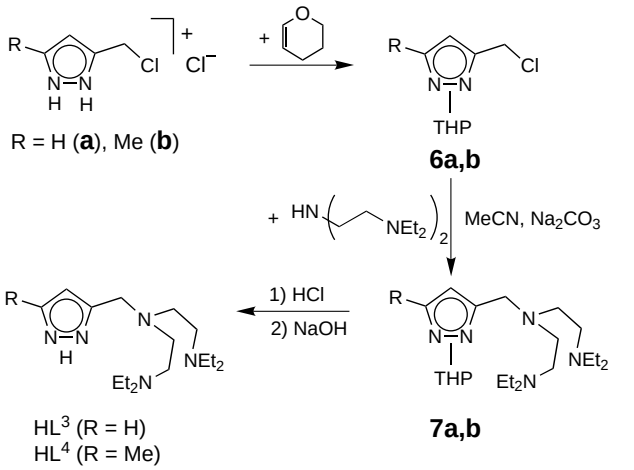

Scheme 4. Mononucleating ligands HL^3 and HL^4, which bear only one donor side arm.

to now.[36, 37] Our synthetic route starts from the 3-(chloromethyl)pyrazole hydrochlorides **6a** and **b** (obtained in two steps from the corresponding esters[38]). For the selective attachment of the polydentate amine side arm by nucleophilic substitution, a NH protecting group had to be introduced at the pyrazole nucleus first. We chose the tetrahydropyran (THP) group, which can easily be removed later from **7a**,**b** by acidification. Owing to their polyamine nature, the resulting potential ligands HL^3 and HL^4 proved difficult to purify by chromatographic methods; however, careful control of the reaction conditions gave material that was sufficiently pure for all subsequent complexation purposes.

Reaction of solutions of HL^3 or HL^4 in MeCN with one equivalent of $[Ni(H_2O)_6](ClO_4)_2$ in the absence of any additional external base afforded blue solutions of complexes **8a** and **b**. These products were obtained in crystalline form by slow diffusion of Et_2O into the reaction mixtures. The formation of coordination compounds was verified by mass spectrometry, which showed dominant signals for $[HL^3Ni(ClO_4)]^+$ and $[HL^4Ni(ClO_4)]^+$. Characteristic bands in the IR spectra of the crystalline material suggested the presence of coordinated MeCN as well as a hydrogen-bonded NH group. However, as already expected from the color, the optical absorption spectra of **8a** and **b** in solution differed fundamentally from those of all dinuclear complexes discussed above (Table 2), but showed weak ligand-field absorptions at 1040 and 575 cm^{-1}, and a shoulder (obscured by intense intraligand absorptions) at around 368 cm^{-1}. These features are diagnostic for six-coordinate high-spin nickel(II) (assigned to the $^3A_{2g} \rightarrow {}^3T_{2g}$, $^3A_{2g} \rightarrow {}^3T_{1g}(F)$, and $^3A_{2g} \rightarrow {}^3T_{1g}(P)$ transitions)[39] and this geometry is indeed preserved in the solid state, as confirmed by an X-ray crystallographic analysis of **8b** (Figure 6). The structure reveals that, apart from the anticipated fourfold coordination of the nickel ion within the tran-type compartment of HL^4, two *cis* binding sites of a distorted overall octahedral coordination sphere are occupied by MeCN solvent molecules. The interatomic distances Ni–N4 [2.293(2) Å] and Ni–N5 [2.273(2) Å] are significantly longer than all equatorial bond lengths within the plane of the pyrazolate (2.013 – 2.094 Å), thus indicating axial elongation

0947-6539/99/0505-1622 $ 17.50+.50/0 *Chem. Eur. J.* **1999**, *5*, No. 5

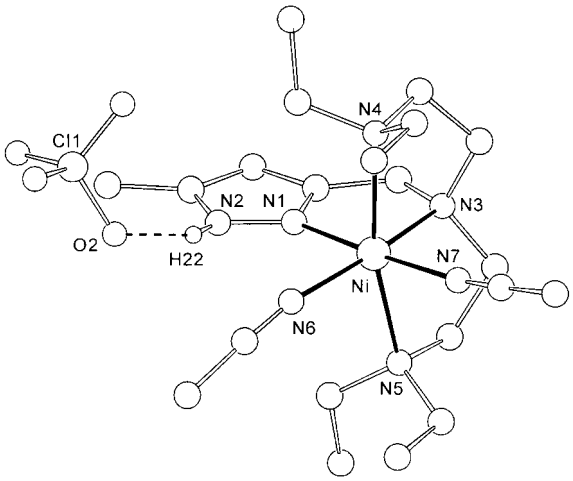

Figure 6. Molecular structure of cation **8b**. In the interests of clarity most of the hydrogen atoms have been omitted. Selected interatomic distances [Å] and bond angles [°]: Ni1–N1 2.013(2), Ni1–N3 2.094(2), Ni1–N4 2.293(2), Ni1–N5 2.273(2), Ni1–N6 2.070(2), Ni1–N7 2.069(3), N1–N2 1.354(3); N1-Ni1-N7 177.0(1), N3-Ni1-N6 169.5(1), N4-Ni-N5 165.0(1).

of the OC–6 environment. The hydrogen atom H22 bound to the pyrazolate N2 atom was located as a bridge to the O2 atom of one of the perchlorate counteranions [d(N2 ··· O2) = 2.972 Å].

In contrast, if a solution of **8a** was treated with base or if the complexation was carried out with the lithiated (deprotonated) ligand LiL^3 and [Ni(H$_2$O)$_6$](ClO$_4$)$_2$, a green complex **9** was formed, which exhibited UV spectroscopic properties similar to those of the bimetallic complexes reported above (Table 2). In addition, the mass spectrum featured dominant signals corresponding to [(L^{3}Ni)$_2$(ClO$_4$)]$^+$ in this case, and no IR spectroscopic evidence for either coordinated acetonitrile or a pyrazolate NH unit could be detected. The cause of these findings was resolved by an X-ray crystallographic analysis of green crystals of **9** (Figure 7) that were obtained by layering a solution of this compound in MeCN with Et$_2$O. The structure illustrates that two L^{3}Ni entities have dimerized by a bridging coordination of both deprotonated pyrazolate heterocycles,

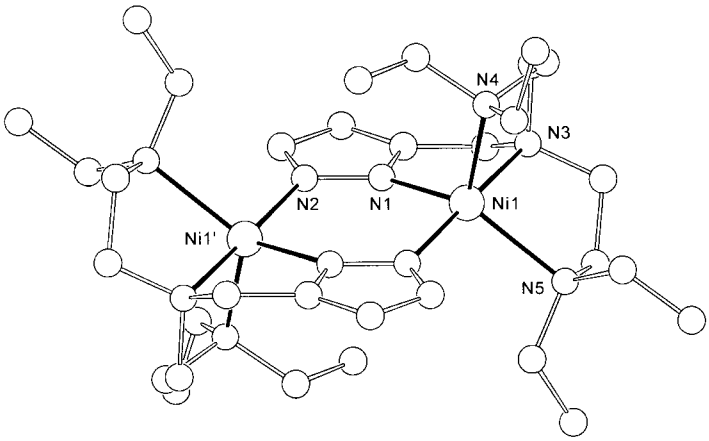

Figure 7. Molecular structure of cation **9**. In the interests of clarity the hydrogen atoms have been omitted. Selected interatomic distances [Å] and bond angles [°]: Ni1–N1 2.034(2), Ni1–N2′ 1.996(2), Ni1–N3 2.122(2), Ni1–N4 2.147(2), Ni1–N5 2.233(2), N1–N2 1.377(2), Ni1 ··· Ni2 4.009; N2′-Ni1-N3 176.31(7), N1-Ni1-N5 134.20(7).

with the dinuclear assembly situated on a crystallographic center of symmetry. The nickel atoms are each coordinated by one L^3 ligand in a tetradentate fashion and adopt an overall fivefold coordination of distinct TB-5 character ($\tau = 0.70$), where the branching N3 atom of one L^3 ligand and the pyrazolate N2 of the second subunit are located in the axial positions. As imposed by the crystallographic restrictions, the two pyrazolate planes are strictly parallel. The distance Ni ··· Ni amounts to 4.009 Å and thus is somewhat longer than the metal–metal separation in several related bis(μ-1,2-pyrazolato)-bridged dinuclear complexes; this is presumably a result of steric constraints of the pyrazolato-linked tran-type ligand compartments which pull the metal centers back and apart (compare with **2** and **1**). Ample precedent exists for the strong tendency of pyrazolate-based multidentate ligand systems to accomplish dimerization by means of 1,2-μ-pyrazolato bridges upon deprotonation of the pyrazole NH, as also observed for **9**.[37]

Interestingly, all *dinuclear* nickel(II) complexes with L^1–L^3 ligand systems described up to this point (in this work and in previous reports[13, 14]) exhibit fivefold coordination with no evidence for any increase in coordination number, either in the solid state (as confirmed by X-ray crystallography) or in solution (based on the optical absorbance spectra). This strongly supports the assumption of a synergetic effect of both nickel ions for the hydration of nitriles by **2** (Scheme 2) or the hydrolysis of other substrates (see below), as only one coordination site is accessible at each metal center, located within the bimetallic pocket of the dinuclear framework. An alternative mechanism would involve binding of both the substrate and the attacking hydroxide at one metal ion (similar to the mechanism of nitrile hydration at some mononuclear complexes[40]) followed by subsequent incorporation of the amidate product into a bridging binding mode within the bimetallic pocket. This appears to be feasible only if additional outer coordination sites are available for substrate binding at the individual metal ions of the bimetallic core. Unexpectedly, the mononuclear complexes **8a** and **b** do indeed feature sixfold coordination, and the binding of the second acetonitrile molecule even appears to be strong, as it could not be removed under dynamic vacuum conditions for prolonged periods. Therefore the alternative mechanism for the nitrile hydration by **2**, which proceeds by an intermediate sixfold coordination of one nickel center due to *exo* substrate binding, has likewise to be kept in mind.

As can be expected for a tran-type nickel(II) complex with two *cis* adjacent coordination sites accessible for substrate binding,[41] the complexes **8a** and **b** are capable of transforming nitriles to the corresponding amides in a catalytic fashion. The presence of a possibly supporting NH-acidic group close to the active metal ion, which has been recognized as a functional principle in many hydrolytic enzymes[1] and has been mimicked in recent model complexes,[42] adds an interesting aspect to these mononuclear systems. A more detailed investigation of their properties and hydrolytic activity will be reported elsewhere.

Hydrolysis of unactivated amides and esters: The proposed mechanism for nitrile hydration, as outlined in Scheme 2,

suggests that the Ni–OH moiety of **2** might, in a similar way, exhibit hydrolase activity towards a variety of other substrates such as esters and amides. Cooperation between two metal ions in functional biomimetic hydrolase models has been an active area of research,[43] which mostly deals with the hydrolytic cleavage of activated *p*-nitrophenyl esters. However, examples for the bimetallic hydrolysis of unactivated carboxyesters and amides have hitherto remained rare.[8, 28]

It turns out that rather high temperatures have to be employed to achieve reasonable rates of reaction of **2** with DMF or DMA. Heating a solution of $\mathbf{2}\cdot(ClO_4)_2$ in either DMF or DMA to 140 °C leads to the formation of the respective carboxylato-bridged complexes **10a** and **b** (Scheme 5), as evidenced by the mass spectra as well as by

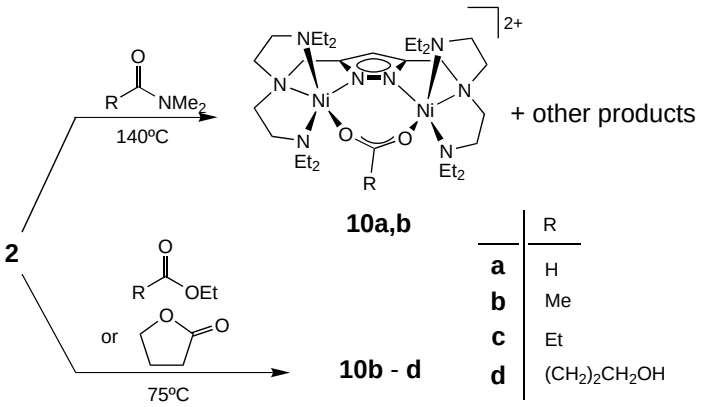

Scheme 5. Formation of the carboxylato-bridged complexes **10a–d**.

the appearance of characteristic strong IR bands for the carboxylato bridges at 1592 cm^{-1} (**10a**) and 1566 cm^{-1} (**10b**) [$\nu_{asym}(CO_2)$; the $\nu_{sym}(CO_2)$ absorptions overlap with other bands and can not be assigned unambiguously]. The identities of these products were confirmed by comparison with identical material prepared independently by treatment of **2** with one equivalent of sodium formate or potassium acetate. However, these hydrolytic cleavages of amides such as DMF and DMA by **2** are sluggish reactions that do not proceed uniformly under the forcing conditions employed, and hence the yields of isolated products **10a** and **b** are low. Unfortunately, no other products could be identified unambiguously.

On the other hand, stoichiometric hydrolysis of the unactivated carboxyesters ethyl acetate and ethyl propionate by **2** runs more cleanly to yield the carboxylato-bridged dinickel(II) complexes **10b** and **c**. They are formed upon heating a suspension of $\mathbf{2}\cdot(ClO_4)_2$ in an excess of the respective carboxyester with subsequent evaporation of all volatile material, as evidenced by the appearance of strong IR features at around 1566 cm^{-1} characteristic for the carboxylate bridges present within the products. The resulting by-product, ethanol, could be detected by GC among the volatile products of the reaction. The identity of **10b** and **c** was further confirmed by mass spectrometry and elemental analyses and by comparison of the physical properties of **10b** with those obtained on a sample synthesized independently from **2** and potassium acetate. In order to definitely exclude the possibility that **10b** and **c** were formed from adventitious traces of free acid or carboxylate within the carboxyester employed, the reactants were first stirred at room temperature for 10 min (conditions that proved to readily yield **10b** from **2** and potassium acetate), and the absence of any carboxylate-bridged product was checked by IR spectroscopy after evaporation of all volatile material. A more detailed follow-up of the course of the hydrolytic transformations by UV/Vis spectroscopy is unfortunately hampered by the only marginal changes in ligand field absorptions during the reactions (Table 2).

The hydrolytic cleavage of the cyclic ester, γ-butyrolactone, upon treatment with $\mathbf{2}\cdot(ClO_4)_2$ proceeds more easily than in the case of the acyclic carboxyesters to yield complex $\mathbf{10d}\cdot(ClO_4)_2$, which contains the liberated HOR function as part of the product molecule. Its identity was verified by spectroscopic and analytical data and by an X-ray crystallographic analysis (Figure 8). The molecular structure of the cation **10d**

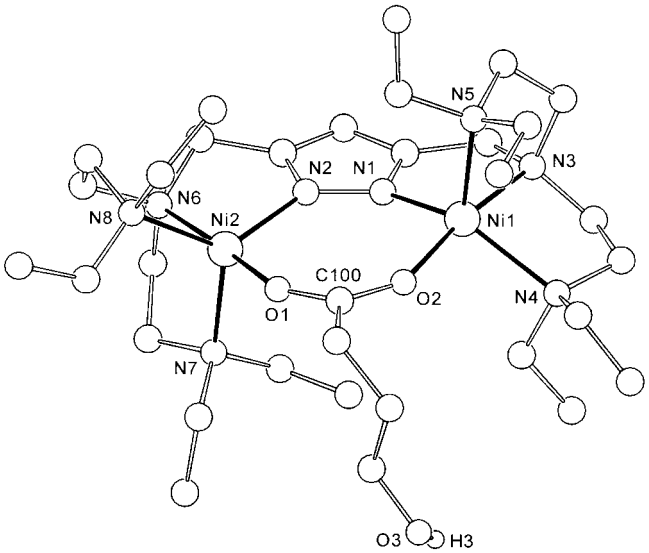

Figure 8. Molecular structure of cation **10d**. In the interests of clarity most of the hydrogen atoms have been omitted. Selected interatomic distances [Å] and bond angles [°]: Ni1–O2 2.022(2), Ni1–N1 2.009(2), Ni1–N3 2.120(2), Ni1–N4 2.165(3), Ni1–N5 2.101(3), Ni2–O1 1.977(2), Ni2–N2 1.993(2), Ni2–N6 2.104(3), Ni2–N7 2.145(3), Ni2–N8 2.176(3), N1–N2 1.374(3), Ni1 ··· Ni2 4.303; O2-Ni1-N3 171.7(1), N1-Ni1-N4 139.9(1), O1-Ni2-N6 173.8(1), N2-Ni2-N7 131.2(2), O1-C100-O2 126.7(3).

confirms the presence of a 4-hydroxybutyrate secondary bridge resulting from the hydrolytic opening of the lactone substrate, which now spans the two nickel centers within the bimetallic cavity. The hydrogen atom of its terminal dangling hydroxo group was located as a hydrogen bridge to the O203 atom of one of the perchlorate counteranions [d(O3 ··· O203) = 2.831 Å]. There is some similarity to the findings for the amidato-bridged compound **3c**: the distance Ni1 ··· Ni2 is 4.303 Å, while the nickel ions are found with coordination geometries of somewhat more pronounced TB-5 character [$\tau = 0.53$ (Ni1) and 0.71 (Ni2)] in **10d**. The interatomic distances Ni1–O2 and Ni2–O1 differ only slightly [2.022(2) versus 1.977(2) Å], which indicates symmetric binding of the carboxylate moiety in accordance with the IR spectroscopic results.

0947-6539/99/0505-1624 $ 17.50+.50/0 *Chem. Eur. J.* **1999**, *5*, No. 5

Hydrolytic cleavage of carboxyesters by **2** as described above is of strictly stoichiometric nature because of the high tendency of the pyrazolate-based dinuclear entities to incorporate secondary bridges within the bimetallic pocket, resulting in inhibition of the active bimetallic site by the hydrolysis product. Nevertheless we were interested as to whether the integrity of the bimetallic framework would persist in the presence of an excess of potentially coordinating carboxylate. Addition of several equivalents of potassium acetate to $\mathbf{2}\cdot(ClO_4)_2$ in fact produced a crystalline compound, $\mathbf{11}\cdot(BPh_4)$, whose IR spectrum was different from that of $\mathbf{10b}\cdot(ClO_4)_2$ but indicated the presence of more than one type of coordinating acetate. On the basis of the small separations of the antisymmetric and symmetric acetate vibrations (1573/1552 and 1447/1408 cm^{-1}) a bidentate coordination mode for both acetate groups could be predicted.[44] The reason for this was elucidated by an X-ray crystallographic analysis (Figure 9). It revealed that besides the expected acetate bridge spanning the two nickel ions, a second acetate anion is coordinated to the Ni1 center in a bidentate fashion, thereby driving out one of the side-arm amino donors of the primary ligand core, which is now found uncoordinated and dangling. The binding of the additional acetate is symmetric [d(N1–O1) = 2.141(3), d(Ni1–O2) = 2.109(3) Å] in accordance with the IR spectroscopic findings. This leads to a distorted octahedral sixfold coordination of Ni1, while the Ni2 center retains the usual fivefold coordination ($\tau = 0.62$). At the same time the Ni···Ni separation is slightly compressed (4.189 Å), which induces considerable tilting of the planar bridging acetate moiety with respect to the plane defined by the pyrazolate heterocycle (42.5°). As a consequence, the two nickel ions are forced to displace rather drastically above and below the pyrazolate plane by the unusually large values of 0.482 Å (Ni1) and 0.701 Å (Ni2).

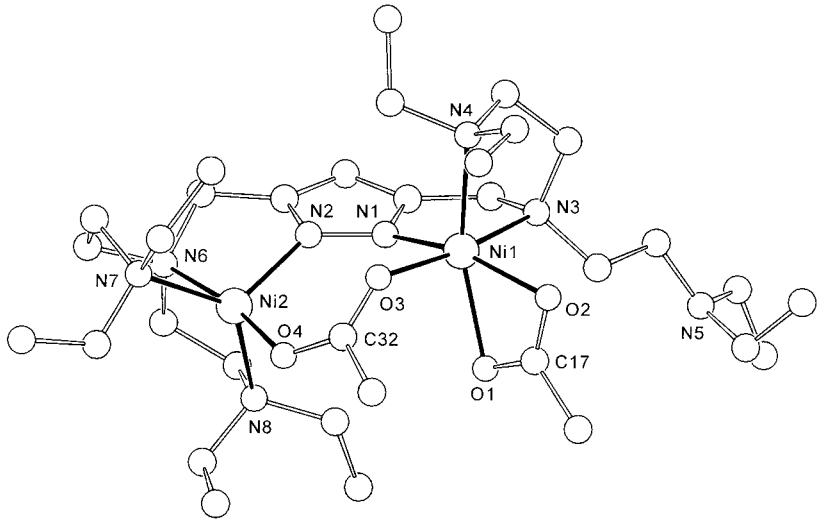

Figure 9. Molecular structure of cation **11**. In the interests of clarity the hydrogen atoms have been omitted. Selected interatomic distances [Å] and bond angles [°]: Ni1–O1 2.141(3), Ni1–O2 2.109(3), Ni1–O3 2.080(3), Ni1–N1 1.994(4), Ni1–N3 2.198(4), Ni1–N4 2.155(4), Ni2–O4 1.991(3), Ni2–N2 1.995(4), Ni2–N6 2.128(4), Ni2–N7 2.155(4), Ni2–N8 2.125(4), N1–N2 1.360(5), Ni1···Ni2 4.189; O1-Ni1-O2 62.1(2), N1-Ni1-O2 162.9(2), N4-Ni1-O1 161.0(2), N3-Ni1-O3 172.0(2), O4-Ni2-N6 170.0(2), N7-Ni2-N8 133.1(2), O1-C17-O2 121.3(5), O3-C32-O4 125.1(5).

The structural findings for **11** could also have implications for the mechanism of the hydrolytic reactions described above, as they may suggest the possibility of an intermediate displacement of a primary ligand side arm by the incoming substrate instead of the anticipated substrate binding within the bimetallic pocket. However, we consider this alternative unlikely because of the much weaker donor strength of the ester or amide substrates compared to an anionic carboxylate.

Conclusions

The suitability of the present pyrazolate-based polyamine ligands to form dinickel(II) complexes that provide a secondary coordination pocket between the two metal centers has been demonstrated, with the metal–metal separation tuneable by appropriate changes of the chain length of the chelating side arms attached to the heterocycle. While the Ni···Ni distance of around 3.5 Å in **1** is similar to that found in the metalloenzyme urease,[5–7] its secondary OH bridge is hydrolytically inactive because of its tight fixation within the grip of the two metal ions. It appears that particular geometric conditions have to prevail within the active site of urease in order to induce hydrolytic attack of a potentially bridging metal-bound water or hydroxide on the urea substrate. This is possibly enabled by favorable preorganization due to a bridging coordination of both the substrate and the nucleophile as suggested recently.[7] In contrast, the H_3O_2 bridge in **2** obtained by pulling the two metal ions back and apart to a Ni···Ni distance of around 4.45 Å is capable of transforming various substrates within the bimetallic pocket, which confirms the description of the H_3O_2 moiety as a resting form of an active metal-bound hydroxide. The most likely mechanism for the hydration of nitriles by **2**, which includes the replacement of a coordinated water fragment of the H_3O_2 bridge by the substrate prior to nucleophilic attack of the well-positioned nickel-bound hydroxide, closely resembles the previously proposed and widely accepted cooperative mechanism for urease activity.[3–6] However, **2** exibits basic rather than nucleophilic properties towards urea, and this leads to a bridging coordination mode of the latter that may have relevance for the more recent mechanistic proposal for the activation of this substrate by the metalloenzyme.[7] Regardless of this, a thermal decomposition pathway of deprotonated bridging urea to form a coordinated cyanate is observed within the tight clinch of the dinickel(II) pincer, related to the slow

uncatalyzed decomposition of urea in aqueous solution. The resulting complex **4** is also accessible directly from **2** and dimethylcyanamide, in accordance with the inability to coordinate any N-substituted urea in a way analogous to parent urea within the bimetallic pocket of the present dinickel(II) complexes.

Unactivated amides and esters likewise undergo stoichiometric hydrolysis by **2**, although this is a sluggish reaction in the former case. The considerable thermal activation necessary to reach reasonable rates of reaction is presumably caused by the strong binding of the water molecule in the H_3O_2 bridge, which counteracts its requisite release for the coordination of the substrate within the bimetallic pocket. Possible alternative mechanisms for these transformations either include an intermediate increase in coordination number at one nickel center due to substrate binding at an additional outer site, or the intermediate displacement of a coordinating ligand side-arm donor by the substrate. Both alternatives still necessitate a break-up of the strongly hydrogen-bridged H_3O_2 unit in order to deliver the nucleophilic nickel-bound hydroxide. While the latter mechanism seems unlikely on the basis of the weak donor strength of the substrates employed (at least in case of esters and amides), the former possibility finds some corroboration in the unexpected sixfold coordination observed for the related mononuclear systems **8a** and **b**. However, no evidence for sixfold coordination of at least one metal ion could be obtained for any *dinuclear* complex of the particular pyrazolate ligand systems used in this or previous work,[13, 14, 15c] either in solution or in the solid state, as long as the ligand side arms are not driven out by more strongly coordinating ligands as in **11**. The present findings thus help to elucidate the factors that determine cooperative reactivity at bimetallic complexes reminiscent of the active sites of natural metalloenzymes like urease, and should eventually assist in the design and generation of more elaborate hydrolytically active hydroxo-dimetal compounds.

Experimental Section

General procedures and methods: All manipulations were carried out under an atmosphere of dry nitrogen with standard Schlenk techniques. Solvents were dried by established procedures. Ligands HL^1 and HL^2 were synthesized according to the reported method.[15c] Microanalyses were performed by the Mikroanalytische Laboratorien des Organisch-Chemischen Instituts der Universität Heidelberg. For compounds containing BPh_4^- ions, the carbon values of the combustion analyses tend to be somewhat low in some cases, presumably due to the formation of intractable boron carbide. IR spectra: Perkin–Elmer 983G, recorded as KBr pellets; FAB-MS spectra: Finnigan MAT 8230; UV/Vis spectra: Perkin–Elmer Lambda 19; cyclic voltammetry: PAR equipment (potentiostat/galvanostat 273), in 0.1 M n-Bu_4NPF_6/MeCN, potentials in V on glassy carbon electrode, referenced to a saturated calomel electrode (SCE) at ambient temperature. NMR spectra: Bruker AC 200 at 200.13 (^{1}H) and 50.32 MHz (^{13}C). Magnetic measurements: Bruker Magnet B-E 15 C8, field-controller B-H 15, variable temperature unit ER4111VT, Sartorius micro balance M 25 D-S. Experimental susceptibility data were corrected for the underlying diamagnetism.

Caution! Although no problems were encountered in this work, transition metal perchlorate complexes are potentially explosive and should be handled with proper precautions.

Complex 1: A solution of HL^1 (0.26 g, 0.56 mmol) in THF (25 mL) and EtOH (1 mL) was treated with two equivalents of LiBu (2.5 M in hexane) and stirred for 5 min at room temperature. All volatile material was removed under reduced pressure and the residue taken up in EtOH (25 mL). $[Ni(H_2O)_6](ClO_4)_2$ (0.41 g, 1.12 mmol) was added in one portion and the resulting green solution was stirred for 15 min. Then $NaBPh_4$ (0.39 g, 1.14 mmol) was added to cause immediate formation of a voluminous light green precipitate. This was filtered off, washed twice with EtOH (10 mL), once with acetone (5 mL), and finally dried under vacuum to yield a light green powder. Vapor diffusion of Et_2O into a solution of this material in MeCN afforded green crystals of $[L^1Ni_2(OH)](BPh_4)_2$, $\mathbf{1}\cdot(BPh_4)_2$ (0.43 g, 0.35 mmol, 62%). IR (KBr): $\tilde{\nu}$ = 3577 (w), 3044 (m), 2973 (s), 2857 (w), 1469 (s), 1454 (s), 1419 (m) cm^{-1}; $C_{73}H_{94}B_2N_8Ni_2O$ (1238.6): calcd C 70.79, H 7.65, N 9.05; found C 70.56, H 7.83, N 8.95.

Complex 2: A solution of HL^2 (0.52 g, 1.00 mmol) in THF (30 mL) and EtOH (1 mL) was treated with two equivalents of LiBu (2.5 M in hexane) and stirred for 5 min at room temperature. The solution was then reduced to a volume of ≈5 mL under reduced pressure. After dilution with EtOH (25 mL), $[Ni(H_2O)_6](ClO_4)_2$ (0.73 g, 2.00 mmol) was added in one portion and the resulting green solution was stirred for 30 min. The reaction mixture was again reduced to a volume of ≈5 mL under reduced pressure. Addition of Et_2O (25 mL) caused formation of a green oil, which was separated by decantation and dried under vacuum. When a solution of this material in acetone was layered with light petroleum, large green crystals of $[L^2Ni_2(O_2H_3)](ClO_4)_2$, $\mathbf{2}\cdot(ClO_4)_2$ (0.65 g, 0.74 mmol, 74%) were obtained. IR (KBr): $\tilde{\nu}$ = 3561 (br m), 3143 (w), 2968 (s), 2871 (m), 1524 (w), 1469 (s), 1381 (m), 1088 (vs) cm^{-1}; MS (FAB, nibeol): m/z (%): 773 (100) [$\mathbf{2}\cdot(ClO_4)^+$], 753 (52) [$L^2Ni_2(OH)(ClO_4)^+$], 672 (50) [$\mathbf{2}^+$]; $C_{29}H_{64}Cl_2N_8Ni_2O_{10}$ (873.2): calcd C 39.89, H 7.39, N 12.83; found C 39.95, H 7.36, N 12.84. Treatment of a solution of $\mathbf{2}\cdot(ClO_4)_2$ (0.40 g, 0.46 mmol) in EtOH with $NaBPh_4$ (0.32 g, 0.94 mmol) caused the immediate formation of a light green precipitate. This was filtered off, washed twice with EtOH (10 mL) and dried under vacuum to give a light green powder. When a solution of this material in acetone was layered with light petroleum, green crystals of $[L^2Ni_2(O_2H_3)](BPh_4)_2(acetone)_2$, $\mathbf{2}\cdot(BPh_4)_2(acetone)_2$ (0.56 g, 0.39 mmol, 85%) were obtained. IR (KBr): $\tilde{\nu}$ = 3440 (br), 3046 (m), 2974 (s), 2872 (m), 1574 (m), 1472 (s), 1420 (m), 1380 (m) cm^{-1}; MS (FAB, nibeol): m/z (%): 672 (100) [$\mathbf{2}^+$]; $C_{83}H_{116}B_2N_8Ni_2O_4$ (1428.9): calcd C 69.77, H 8.18, N 7.84; found C 70.34, H 8.57, N 7.76.

Complex 3a: A solution of $\mathbf{2}\cdot(ClO_4)_2$ (0.26 g, 0.30 mmol) in MeCN (2 mL) was heated to 75 °C for 12 h. After cooling to room temperature, the solvent was evaporated under reduced pressure, and the residue taken up in acetone and layered with light petroleum to yield green crystals of $[L^2Ni_2\{O(NH)CMe\}](ClO_4)_2$, $\mathbf{3a}\cdot(ClO_4)_2$ (0.24 g, 0.27 mmol, 89%); IR (KBr): $\tilde{\nu}$ = 3329 (m), 2973 (s), 2871 (s), 1572 (s), 1477 (s), 1379 (m), 1087 (vs) cm^{-1}; MS (FAB, nibeol): m/z (%): 796 (100) [$\mathbf{3a}\cdot(ClO_4)^+$], 695 (28) [$\mathbf{3a}^+$]; $C_{31}H_{65}Cl_2N_9Ni_2O_9$ (896.2): calcd C 41.55, H 7.31, N 14.07; found C 41.44, H 7.16, N 13.95. Identical material was obtained by treating $\mathbf{2}\cdot(ClO_4)_2$ with one equivalent of acetamide in acetone. Complex $\mathbf{3a}\cdot(BPh_4)_2$ was prepared by an analogous procedure from $\mathbf{2}\cdot(BPh_4)_2$. Crystalline material was obtained by layering a solution of the product in MeCN with Et_2O. IR (KBr): $\tilde{\nu}$ = 3440 (br), 3048 (m), 2975 (s), 2873 (w), 1575 (s), 1472 (s), 1421 (m), 1380 (m) cm^{-1}; MS (FAB, nibeol): m/z (%): 695 (100) [$\mathbf{3a}^+$]; $C_{79}H_{105}B_2N_9Ni_2O$ (1335.8): calcd C 71.04, H 7.92, N 9.44; found C 69.31, H 7.92, N 10.12.

Complex 3b: The synthesis was carried out analogously to that of **3a** from $\mathbf{2}\cdot(ClO_4)_2$ (0.26 g, 0.30 mmol) and acrylonitrile (2 mL). Green microcrystals were obtained when a solution of the product $[L^2Ni_2\{O(NH)CC_2H_3\}](ClO_4)_2$, $\mathbf{3b}\cdot(ClO_4)_2$, in acetone was overlayed with light petroleum (0.22 g, 0.24 mmol, 81%). IR (KBr): $\tilde{\nu}$ = 3306 (m), 2969 (s), 2875 (s), 1630 (m), 1546 (s), 1467 (s), 1390 (m), 1379 (m), 1092 (vs) cm^{-1}; MS (FAB, nibeol): m/z (%): 808 (100) [$\mathbf{3b}\cdot(ClO_4)^+$], 707 (33) [$\mathbf{3b}^+$], 354 (10) [$\mathbf{3b}^{2+}$]; $C_{32}H_{65}Cl_2N_9Ni_2O_9$ (908.2): calcd C 42.32, H 7.21, N 13.88; found C 42.01, H 7.11, N 13.63.

Complex 3c: The synthesis was carried out analogously to that of **3a** from $\mathbf{2}\cdot(ClO_4)_2$ (0.26 g, 0.30 mmol) and benzonitrile (2 mL). Green crystals were obtained when a solution of the product $[L^2Ni_2\{O(NH)CPh\}](ClO_4)_2$, $\mathbf{3c}\cdot(ClO_4)_2$, in acetone was overlayed with light petroleum (0.23 g, 0.24 mmol, 80%). IR (KBr): $\tilde{\nu}$ = 3362 (w), 2974 (m), 2876 (m), 1663 (w), 1586 (s), 1549 (s), 1454 (s), 1380 (m) cm^{-1}; MS (FAB, nibeol): m/z (%): 858 (100) [$\mathbf{3c}\cdot$

0947-6539/99/0505-1626 $ 17.50+.50/0 *Chem. Eur. J.* **1999**, *5*, No. 5

$(ClO_4)^+$], 757 (30) [**3c**$^+$], 679 (22) [**3c**$^+ - C_6H_6$]; $C_{36}H_{67}Cl_2N_9Ni_2O_9$ (958.3): calcd C 45.12, H 7.05, N 13.15; found C 44.67, H 7.10, N 13.04.

Complex 4: **a) from 2 and dimethylcyanamide**: A solution of **2**·$(ClO_4)_2$ (0.26 g, 0.30 mmol) in dimethylcyanamide (2 mL) was heated to 70 °C for 12 h. Most of the volatile material was then evaporated under reduced pressure and the residue taken up in EtOH (15 mL). Addition of $NaBPh_4$ (0.21 g, 0.61 mmol) caused immediate formation of a light green precipitate which was filtered, washed twice with EtOH, and dried under vacuum. When a solution of the resulting product in acetone was layered with light petroleum, green crystals of [$L^2Ni_2(OCN)$]$(BPh_4)_2$(acetone), **4**·$(BPh_4)_2$·(acetone) (0.27 g, 0.20 mmol, 65 %) were obtained. IR (KBr): $\tilde{\nu} = 3047$ (m), 2976 (s), 2876 (w), 2217 (s), 2201(s), 1572 (m), 1469 (s), 1446 (m), 1419 (m), 1380 (m) cm^{-1}; MS (FAB, nibeol): *m*/*z* (%): 679 (100) [**4**$^+$]; $C_{78}H_{101}B_2N_9Ni_2O$·acetone (1377.8): calcd C 70.61, H 7.83, N 9.15; found C 69.98, H 8.14, N 8.64.

b) from 5: A powdered sample of neat **5**·$(ClO_4)_2$ (0.22 g, 0.25 mmol) was placed in a Schlenk tube and heated to 170 °C while being stirred under dynamic vacuum. Occasionally samples were taken to monitor the appearance of the band at 2195 cm^{-1} by IR spectroscopy, characteristic of product formation. After 12 h the resulting material was cooled to room temperature, taken up in acetone (7 mL) and filtered. When the green solution was layered with light petroleum, green microcrystals of [$L^2Ni_2(OCN)$]$(ClO_4)_2$, **4**·$(ClO_4)_2$ (0.14 g, 0.16 mmol, 65 %) slowly formed. IR (KBr): $\tilde{\nu} = 2975$ (m), 2877 (w), 2193 (s), 1465 (sh), 1453 (m), 1384 (m), 1088 (vs) cm^{-1}; MS (FAB, nibeol): *m*/*z* (%): 780 (100) [**4**·$(ClO_4)^+$], 679 (50) [**4**$^+$]; $C_{30}H_{61}Cl_2N_9Ni_2O_9$ (880.2): calcd C 40.94, H 6.99, N 14.32; found C 40.72, H 7.15, N 14.15. Anion exchange with $NaBPh_4$ yielded material with physical properties identical to those of [$L^2Ni_2(OCN)$]$(BPh_4)_2$ obtained from the reaction of **2**·$(ClO_4)_2$ and dimethylcyanamide described above.

Ligand HL^3: 3-Chloromethylpyrazole hydrochloride was prepared according to the literature.[38] ^{1}H NMR ([D$_6$]DMSO): $\delta = 4.72$ (s, 2H, CH_2), 6.34 (d, $J = 1.8$ Hz, 1H, H^4), 7.70 (d, $J = 1.8$ Hz, 1H H^5), 9.09 (br, 2H, NH); ^{13}C NMR ([D$_6$]DMSO): $\delta = 38.5$ (CH_2), 104.8 (C^4), 131.4 (C^5), 146.1 (C^3). A solution of this material (3.0 g, 19.6 mmol) in CH_2Cl_2 (200 mL) was treated with 3,4-dihydropyran (3.6 mL, 39.5 mmol) and stirred at room temperature overnight. After evaporation of all volatile material, the residue was recrystallized from CH_2Cl_2:light petroleum (1:20) at −20 °C to yield **6a** (2.6 g, 13.0 mmol, 66 %) as a sticky white solid. MS (EI): *m*/*z* (%): 201 (5) [M^++1], 85 (100) [THP$^+$]; $C_9H_{13}ClN_2O$ (200.7): calcd C 53.87, H 6.53, N 13.96; found C 54.56, H 6.69, N 12.99. This material and Na_2CO_3 (14 g, 132 mmol; previously dried by heating to 100 °C under dynamic vacuum for 1 h) were added to a solution of bis[(diethylamino)ethyl]amine (2.8 g, 13.0 mmol) in MeCN (200 mL) and the reaction mixture was refluxed for 18 h. After cooling to room temperature and subsequent filtration, the resulting clear solution was evaporated to dryness to yield crude **7a** as a slightly yellow oil. This was taken up in ethanolic HCl (40 mL) and stirred for 1 h at room temperature. The volume of the solution was reduced to 30 mL under reduced pressure and addition of ether precipitated the product as the hydrochloride salt, which was separated by decantation and dried under vacuum. Aqueous NaOH (1M, 70 mL) was added and extracted twice with CH_2Cl_2. The combined organic phases were dried over $MgSO_4$ and evaporated to dryness to afford HL^3 (1.7 g, 5.8 mmol, 44 %) as a slightly yellow oil. ^{1}H NMR ($CDCl_3$): $\delta = 1.06$ (t, $J = 7.1$ Hz, 12H, CH_3), 2.45–2.67 (m, 16H, CH_2), 3.80 (s, 2H, CH_2), 6.01 (d, $J = 1.6$ Hz, 1H, H^4), 7.48 (d, $J = 1.6$ Hz, H^5); ^{13}C NMR ($CDCl_3$): $\delta = 11.4$ (CH_3), 47.1, 49.5, 51.5, 53.4 (CH_2), 101.6 (C^4), 127.9 (C^5), 139.1 (C^3); MS (EI): *m*/*z* (%): 294 (5) [$M^+ - 1$], 209 (12) [$M^+ - CH_2NEt_2$], 86 (100) [$CH_2NEt_2^+$].

Ligand HL^4: The preparation was carried out in close analogy to that of HL^3 from 3-chloromethyl-5-methylpyrazole hydrochloride.[38] ^{1}H NMR ([D$_6$]DMSO): $\delta = 2.25$ (s, 3H, CH_3), 4.70 (s, 2H, CH_2), 6.22 (s, 1H, H^4); ^{13}C NMR ([D$_6$]DMSO): $\delta = 10.7$ (CH_3), 37.8 (CH_2), 104.5 (C^4), 141.8 (C^5), 146.1 (C^3). Compound **6b** was obtained as a mixture of isomers and was finally converted to HL^4 as a slightly yellow oil (overall yield 37 %). ^{1}H NMR ($CDCl_3$): $\delta = 1.05$ (t, $J = 7.1$ Hz, 12H, CH_3), 2.27 (s, 3H, CH_3), 2.48–2.66 (m, 16H, CH_2), 3.73 (s, 2H, CH_2), 5.80 (s, 1H, H^4); ^{13}C NMR ($CDCl_3$): $\delta = 11.2$ (CH_3), 13.1 (CH_3), 47.2, 49.6, 51.4, 53.4 (CH_2), 101.5 (C^4), C^5/C^3 not observed; MS (FAB, nibeol): *m*/*z* (%): 310 (100) [M^++1], 223 (61) [$M^+ - CH_2NEt_2$].

Complex 8a: One equivalent of $[Ni(H_2O)_6](ClO_4)_2$ (0.22 g, 0.61 mmol) was added to a solution of HL^3 (0.18 g, 0.61 mmol) in MeCN (20 mL) and the resulting blue solution stirred for 2 h at room temperature. After the volume of the reaction mixture was reduced to ≈8 mL under reduced pressure, it was layered with Et_2O. Blue-violet crystals of [$HL^3Ni(NCMe)_2$]$(ClO_4)_2$, **8a**·$(ClO_4)_2$, gradually formed (0.17 g, 0.27 mmol, 44 %). IR (KBr): $\tilde{\nu} = 3131$ (w), 2979 (m), 2877 (w), 2311 (m), 2287 (m), 2248 (m), 1529 (m), 1461 (s), 1391 (m), 1090 (vs) cm^{-1}; MS (FAB, nibeol): *m*/*z* (%): 452 (90) [**8a**·$(ClO_4)^+ - 2$MeCN], 353 (100) [**8a**$^+ - 2$MeCN]; $C_{20}H_{39}Cl_2N_7NiO_8$ (635.2): calcd C 37.82, H 6.19, N 15.44; found C 38.10, H 6.14, N 15.91.

Complex 8b: This was prepared analogously to **8a** from HL^4 (0.19 g, 0.61 mmol) to yield blue-violet crystals of [$HL^4Ni(NCMe)_2$]$(ClO_4)_2$, **8b**·$(ClO_4)_2$ (0.19 g, 0.29 mmol, 48 %). IR (KBr): $\tilde{\nu} = 3140$ (vw), 2980 (m), 2877 (w), 2304 (m), 2278 (m), 1568 (m), 1468 (m), 1446 (m), 1392 (w), 1090 (vs) cm^{-1}; MS (FAB, nibeol): *m*/*z* (%): 466 (100) [**8b**·$(ClO_4)^+ - 2$MeCN], 366 (39) [**8a**$^+ - 2$MeCN]; $C_{21}H_{41}Cl_2N_7NiO_8$ (649.2): calcd C 38.85, H 6.37, N 15.10; found C 38.57, H 6.30, N 14.95.

Complex 9: One equivalent of BuLi (2.5M in hexane) was added to a solution of HL^3 (0.18 g, 0.61 mmol) in THF (20 mL). After the volume of the solution was reduced to ≈10 mL under vacuum with subsequent addition of MeCN (10 mL), $[Ni(H_2O)_6](ClO_4)_2$ (0.22 g, 0.61 mmol) was added in one portion and the resulting green solution was stirred for 3 h at room temperature. All volatile material was then removed under reduced pressure and the remaining material taken up in MeCN and layered with Et_2O. Green crystals of [$L^3{}_2Ni_2$]$(ClO_4)_2$, **9**·$(ClO_4)_2$, gradually formed (0.23 g, 0.25 mmol, 83 %). IR (KBr): $\tilde{\nu} = 2958$ (m), 1461 (m), 1379 (m), 1335 (m), 1258 (s), 1090 (vs) cm^{-1}; MS (FAB, nibeol): *m*/*z* (%): 805 (100) [**9**·$(ClO_4)^+$], 704 (73) [**9**$^+$], 352 (79) [L^3Ni^+]; $C_{32}H_{64}Cl_2N_{10}Ni_2O_8$ (905.2): calcd C 42.46, H 7.13, N 15.47; found C 42.26, H 6.99, N 15.45.

Complex 10a: **a) by hydrolysis of DMF**: A solution of **2**·$(ClO_4)_2$ (0.30 g, 0.34 mmol) in DMF (2 mL) was heated to 140 °C for 36 h. All volatile material was then removed under reduced pressure at 30 °C and the residue dissolved in EtOH (25 mL). Addition of $NaBPh_4$ (0.24 g, 0.70 mmol) caused precipitation of a green solid which was filtered off and washed twice with small portions of EtOH. When a solution of this material in acetone was layered with light petroleum, microcrystalline green [$L^2Ni_2(O_2CH)$]$(BPh_4)_2$(acetone), **10a**·$(BPh_4)_2$(acetone) (0.19 g, 0.14 mmol, 40 %), was obtained. IR (KBr): $\tilde{\nu} = 3047$ (m), 2975 (s), 2872 (w), 1704 (s, acetone), 1592 (s), 1574 (s), 1473 (s), 1444 (m), 1420 (m), 1380 (m) cm^{-1}; MS (FAB, nibeol): *m*/*z* (%): 682 (100) [**10a**$^+$]; $C_{78}H_{102}B_2N_8Ni_2O_2$·acetone (1380.8): calcd C 70.46, H 7.88, N 8.12; found C 69.73, H 7.56, N 8.34.

b) from 2 and formate: Identical material was obtained by treating a solution of **2**·$(ClO_4)_2$ (0.20 g, 0.23 mmol) in EtOH (20 mL) with sodium formate (0.017 g, 0.23 mmol) and subsequent anion exchange with $NaBPh_4$ (0.16 g, 0.46 mmol). Crystallization from acetone/light petroleum afforded green crystalline **10a**·$(BPh_4)_2$(acetone) (0.28 g, 0.20 mmol, 88 %); MS (FAB, nibeol): *m*/*z* (%): 682 (100) [**10a**$^+$]; $C_{78}H_{102}B_2N_8Ni_2O_2$·acetone (1380.8): calcd C 70.46, H 7.88, N 8.12; found C 69.11, H 7.75, N 8.59.

Complex 10b: **a) by hydrolysis of DMA**: A solution of **2**·$(ClO_4)_2$ (0.30 g, 0.34 mmol) in DMA (2 mL) was heated to 140 °C for 36 h. All volatile material was then removed under reduced pressure at 30 °C and the residue washed twice with small portions of Et_2O. Crystallization of the remaining material from MeOH/Et_2O afforded green microcrystals of [$L^2Ni_2(O_2CMe)$]$(ClO_4)_2$, **10b**·$(ClO_4)_2$ (0.09 g, 0.10 mmol, 28 %). IR (KBr): $\tilde{\nu} = 2972$ (m), 2876 (m), 1575 (s), 1449 (br m), 1427 (m), 1384 (m), 1094 (vs) cm^{-1}; MS (FAB, nibeol): *m*/*z* (%): 797 (100) [**10b**·$(ClO_4)^+$], 696 (25) [**10b**$^+$]; $C_{31}H_{64}Cl_2N_8Ni_2O_{10}$ (897.2): calcd C 41.50, H 7.19, N 12.49; found C 40.36, H 7.10, N 12.38. Alternatively, the raw material was taken up in EtOH (25 mL) and treated with $NaBPh_4$ (0.22 g, 0.64 mmol) to yield a green precipitate. This was washed twice with EtOH, dissolved in acetone and layered with light petroleum to afford green microcrystalline **10b**·$(BPh_4)_2$(acetone)$_2$ (0.20 g, 0.14 mmol, 41 %). IR (KBr): $\tilde{\nu} = 3048$ (m), 2975 (s), 2873 (w), 1705 (s, acetone), 1572 (s), 1566 (s), 1468 (s), 1444 (m), 1423 (s), 1381(m), 1354 (m) cm^{-1}; MS (FAB, nibeol): *m*/*z* (%): 696 (100) [**10b**$^+$]; $C_{79}H_{104}B_2N_8Ni_2O_2$·2 acetone (1452.9): calcd C 70.27, H 8.05, N 7.71; found C 70.17, H 7.84, N 7.99.

b) from 2 and acetate: Identical material was obtained by treating a solution of **2**·$(ClO_4)_2$ (0.20 g, 0.23 mmol) in EtOH (20 mL) with potassium acetate (.023 g, 0.23 mmol) and subsequent anion exchange with $NaBPh_4$ (0.16 g, 0.46 mmol). Crystallization from acetone/light petroleum afforded green crystalline **10b**·$(BPh_4)_2$(acetone)$_2$ (0.25 g, 0.17 mmol, 75 %) with physical properties identical to those of the above compound.

c) By hydrolysis of ethyl acetate: A suspension of $\mathbf{2}\cdot(ClO_4)_2$ (0.30 g, 0.34 mmol) in ethyl acetate (3 mL) was heated under reflux for 12 h. All volatile material was then removed under reduced pressure, the residue was dissolved in EtOH and $NaBPh_4$ (0.22 g, 0.64 mmol) added. The green precipitate that formed was filtered and washed twice with EtOH. When a solution of this material in acetone was layered with light petroleum, green microcrystals of $\mathbf{10b}\cdot(BPh_4)_2(acetone)_2$ (0.31 g, 0.21 mmol, 63%) were obtained. MS (FAB, nibeol): *m/z* (%): 696 (100) [$\mathbf{10b}^+$]; $C_{79}H_{104}B_2N_8Ni_2O_2\cdot 2$acetone (1452.9): calcd C 70.27, H 8.05, N 7.71; found C 69.62, H 8.23, N 7.88.

Complex 10c: A suspension of $\mathbf{2}\cdot(ClO_4)_2$ (0.30 g, 0.34 mmol) in ethyl propionate (3 mL) was heated to 75 °C for 12 h. All volatile material was then removed under reduced pressure, and the residue was dissolved in acetone and overlayed with light petroleum. Green microcrystals of the product $[L^2Ni_2(O_2CEt)](ClO_4)_2$, $\mathbf{10c}\cdot(ClO_4)_2$, gradually formed (0.23 g, 0.25 mmol, 74%). IR (KBr): $\tilde{\nu}=2974$ (s), 2876 (m), 1565 (vs), 1516 (w), 1459 (s), 1420 (s), 1384 (m), 1092 (vs) cm^{-1}; MS (FAB, nibeol): *m/z* (%): 809 (100) [$\mathbf{10c}\cdot(ClO_4)^+$], 710 (28) [$\mathbf{10c}^+$]; $C_{32}H_{66}Cl_2N_8Ni_2O_{10}$ (911.2): calcd C 42.18, H 7.30, N 12.30; found C 41.84, H 7.25, N 12.28.

Complex 10d: A solution of $\mathbf{2}\cdot(ClO_4)_2$ (0.30 g, 0.34 mmol) in γ-butyrolactone (2 mL) was heated to 75 °C for 3 h. All volatile material was then removed under reduced pressure, the residue dissolved in acetone and overlayed with light petroleum. Green crystals of the product $\{L^2Ni_2[O_2C(CH_2)_3OH]\}(ClO_4)_2$, $\mathbf{10d}\cdot(ClO_4)_2$, gradually formed (0.27 g, 0.29 mmol, 84%). IR (KBr): $\tilde{\nu}=3518$ (br m), 2973 (s), 2874 (m), 1565 (s), 1445 (s), 1414 (s), 1379 (m), 1082 (vs) cm^{-1}; MS (FAB, nibeol): *m/z* (%): 841 (100) [$\mathbf{10d}\cdot(ClO_4)^+$], 741 (55) [$\mathbf{10d}^+$]; $C_{33}H_{68}Cl_2N_8Ni_2O_{11}$ (941.2): calcd C 42.11, H 7.28, N 11.90; found C 41.82, H 7.17, N 11.76.

Complex 11: A solution of $\mathbf{2}\cdot(BPh_4)_2$ (0.49 g, 0.34 mmol) in acetone (20 mL) was treated with potassium acetate (0.09 g, 0.92 mmol) and stirred at room temperature for 6 h. All volatile material was then removed under reduced pressure, the residue again dissolved in acetone and filtered. When the resulting solution was layered with light petroleum, green crystals of the product $[L^2Ni_2(O_2CCH_3)_2](BPh_4)\cdot(acetone)_{0.6}$, $\mathbf{11}\cdot(BPh_4)(acetone)_{0.6}$ (0.20 g, 0.18 mmol, 52%) were obtained. IR (KBr): $\tilde{\nu}=3046$ (m), 2969 (s), 2868 (m), 1708 (m, acetone), 1573 (vs), 1552 (sh), 1447 (s), 1418 (m), 1408 (s), 1376 (m) cm^{-1}; MS (FAB, nibeol): *m/z* (%): 755 (55) [$\mathbf{11}^+$], 696 (55) [$\mathbf{11}^+ - O_2CCH_3$]; $C_{57}H_{87}BN_8Ni_2O_4\cdot 0.6$ acetone (1111.4): calcd C 63.55, H 8.22, N 10.08; found C 62.26, H 7.92, N 9.68.

X-ray crystallography: The measurements were carried out on a Siemens P4 four-circle diffractometer [complex $\mathbf{1}\cdot(BPh_4)_2$] or a Siemens CCD diffractometer [complex $\mathbf{2}\cdot(BPh_4)_2$] or a Nonius Kappa CCD diffractometer [complexes $\mathbf{3c}\cdot(ClO_4)_2$, $\mathbf{4}\cdot(BPh_4)_2$, $\mathbf{8b}\cdot(ClO_4)_2$, $\mathbf{9}\cdot(ClO_4)_2$, $\mathbf{10d}\cdot(ClO_4)_2$, $\mathbf{11}\cdot(BPh_4)$] with graphite-monochromated $Mo_{K\alpha}$ radiation. For $\mathbf{1}\cdot(BPh_4)_2$ the intensities of three reference reflections (measured every 100 reflections) remained constant throughout the data collection, which indicated crystal and electronic stability. All calculations were performed with the SHELXT PLUS software package. Structures were solved by direct methods with the SHELXS-97 and refined with the SHELXL-97 program.[45] The program XPMA[46] was used for graphical handling of the data. For $\mathbf{1}\cdot(BPh_4)_2$ an absorption correction (ψ scan, $\Delta\psi=10^\circ$) was applied to the data. Atomic coordinates and thermal parameters of the non-hydrogen atoms were refined in fully or partially anisotropic models by full-matrix least-squares calculation based on F^2. In general, the hydrogen atoms were placed at calculated positions and allowed to ride on the atoms they are attached to. In the case of $\mathbf{2}\cdot(BPh_4)_2$, the hydrogen atoms H100, H200, and H300 of the H_3O_2 bridge were located in the difference fourier synthesis and refined isotropically. The same is valid for the N-bound H22 in $\mathbf{8b}\cdot(ClO_4)_2$ and for the O-bound H3 in $\mathbf{10d}\cdot(ClO_4)_2$. Owing to the poor quality of the crystals, the structure analysis of **4** could only be refined to a final (poor) agreement value of R = 0.105. The data for the structure determinations is compiled in Tables 3 and 4. Crystallographic data (excluding structure factors) for the structures reported in this paper have been deposited with the Cambridge Crystallographic Data Centre as supplementary publication nos. CCDC-111410 – CCDC-111417. Copies of the data can be obtained free of charge on application to CCDC, 12 Union Road, Cambridge CB2 1EZ, UK (fax: (+44) 1223-336-033; e-mail: deposit@ccdc.cam.ac.uk).

Acknowledgements

We are grateful to Prof. Dr. G. Huttner for his generous and continuous support of our work. Financial support by the Deutsche Forschungsgemeinschaft (Habilitandenstipendium for F.M.) and the Fonds der Chemischen Industrie is gratefully acknowledged.

Table 3. Crystal structure data and refinement details for complexes **1**, **2**, **3c**, and **4**.

	$\mathbf{1}\cdot(BPh_4)_2$	$\mathbf{2}\cdot(BPh_4)_2\cdot 2$acetone	$\mathbf{3c}\cdot(ClO_4)_2$	$\mathbf{4}\cdot(BPh_4)_2\cdot$acetone
formula	$C_{73}H_{94}B_2N_8Ni_2O$	$C_{77}H_{104}B_2N_8Ni_2O_2\cdot 2C_3H_6O$	$C_{36}H_{67}Cl_2N_9Ni_2O_9$	$C_{78}H_{101}B_2N_9Ni_2O\cdot C_3H_6O$
M_r	1238.6	1428.9	958.3	1377.8
crystal size [mm]	$0.40\times0.40\times0.50$	$0.24\times0.30\times0.36$	$0.20\times0.20\times0.30$	$0.20\times0.15\times0.15$
crystal system	triclinic	monoclinic	monoclinic	monoclinic
space group	$P\bar{1}$	$P2_1/c$	$P2_1/n$	$P2_1/n$
a [Å]	11.725(2)	12.426(1)	14.956(3)	12.508(3)
b [Å]	14.629(2)	12.778(1)	19.683(4)	21.335(4)
c [Å]	20.095(3)	49.439(1)	15.197(3)	28.858(6)
α [°]	100.53(1)	90	90	90
β [°]	100.21(1)	93.60(1)	107.86(3)	94.06(3)
γ [°]	100.78(1)	90	90	90
V [Å^3]	3248(1)	7834(1)	4258(1)	7682(3)
ρ_{calcd} [g cm^{-3}]	1.266	1.211	1.454	1.177
Z	2	4	4	4
F(000) [e]	1324	3072	1928	2888
T [K]	200	200	200	200
μ ($Mo_{K\alpha}$) [mm^{-1}]	0.631	0.53	1.071	0.541
hkl range	-13 to 14, -17 to 16, -24 to 23	±15, ±14, ±56	±18, ±24, ±18	-13 to 12, ±26, ±35
2θ range [°]	3.6 – 51.0	3.2 – 51.4	3.3 – 52.1	3.4 – 52.0
measured refl.	12662	60049	71810	78539
unique refl. (R_{int})	12035 (0.032)	13689 (0.037)	8419 (0.096)	13835 (0.269)
observed refl. $I>2\sigma(I)$	9074	10892	5469	4675
refined parameters	788	914	583	528
resid. electron dens. [e Å^{-3}]	0.588/ -0.450	1.25/ -0.38	1.35/ -0.69	0.856/ -0.550
R1	0.044	0.053	0.056	0.105
wR2 (refinement on F^2)	0.105	0.131	0.168	0.336
goodness-of-fit	1.024	1.085	0.989	0.960

0947-6539/99/0505-1628 $ 17.50+.50/0 *Chem. Eur. J.* **1999**, *5*, No. 5

Table 4. Crystal structure data and refinement details for complexes **8b**, **9**, **10d**, and **11**.

	8b · $(ClO_4)_2$	**9** · $(ClO_4)_2$	**10d** · $(ClO_4)_2$	**11** · (BPh_4) · 0.6 acetone
formula	$C_{21}H_{41}Cl_2N_7NiO_8$	$C_{32}H_{64}Cl_2N_{10}Ni_2O_8$	$C_{33}H_{68}Cl_2N_8Ni_2O_{11}$	$C_{57}H_{87}BN_8Ni_2O_4 \cdot C_{1.8}H_{3.6}O_{0.6}$
M_r	649.2	905.2	941.2	1111.4
crystal size [mm]	0.20 × 0.20 × 0.05	0.02 × 0.20 × 0.20	0.03 × 0.03 × 0.02	0.02 × 0.01 × 0.01
crystal system	monoclinic	monoclinic	monoclinic	monoclinic
space group	$P2_1/c$	$P2_1/n$	$P2_1/c$	$P2_1/c$
a [Å]	16.728(3)	9.181(2)	17.972(4)	15.938(3)
b [Å]	9.630(2)	12.725(3)	13.112(3)	12.933(3)
c [Å]	18.943(4)	17.253(4)	19.463(4)	29.939(6)
α [°]	90	90	90	90
β [°]	108.70(3)	92.07(3)	114.11(3)	103.05(3)
γ [°]	90	90	90	90
V [Å^3]	2890(1)	2014(1)	4186(1)	6012(2)
ρ_{calcd} [g cm^{-3}]	1.492	1.493	1.493	1.224
Z	4	2	4	4
F(000) [e]	1368	960	2000	2374
T [K]	200	200	200	200
μ ($Mo_{K\alpha}$) [mm^{-1}]	0.912	1.128	1.092	0.678
hkl range	±20, ±11, ±23	±11, ±15, ±21	−22 to 18, ±16, −20 to 23	±19, ±15, −36 to 37
2θ range [°]	4.4–52.2	4.0–52.0	3.9–52.1	4.1–52.2
measured refl.	51579	29681	26873	74099
unique refl (R_{int})	5697 (0.138)	3985 (0.083)	8099 (0.079)	11843 (0.117)
observed refl. $I > 2\sigma(I)$	3138	3215	5555	6190
refined parameters	366	251	519	510
resid. electron dens. [e Å^{-3}]	0.371/−0.367	0.363/−0.342	0.505/−0.372	0.922/−0.698
R1	0.042	0.034	0.046	0.062
wR2 (refinement on F^2)	0.072	0.083	0.098	0.196
goodness-of-fit	0.889	1.039	0.999	1.033

[1] N. Sträter, W. N. Lipscomb, T. Klabunde, B. Krebs, *Angew. Chem.* **1996**, *108*, 2158–2191; *Angew. Chem. Int. Ed. Engl.* **1996**, *35*, 2024–2055.
[2] T. A. Steitz, J. A. Steitz, *Proc. Natl. Acad. Sci. USA* **1993**, *90*, 6498–6502.
[3] N. E. Dixon, P. W. Riddles, C. Gazzola, R. L. Blakeley, B. Zerner, *Can. J. Biochem.* **1980**, *58*, 1335–1344.
[4] a) R. K. Andrews, R. L. Blakeley, B. Zerner, in *The Bioinorganic Chemistry of Nickel* (Ed.: J. R. Lancaster, Jr.), VCH, New York, **1988**; b) A. F. Kolodziej, *Progr. Inorg. Chem.* **1994**, *41*, 493–597; c) M. A. Halcrow, G. Christou, *Chem. Rev.* **1994**, *94*, 2421–2481.
[5] a) E. Jabri, M. B. Carr, R. P. Hausinger, P. A. Karplus, *Science* **1995**, *268*, 998–1004; b) S. J. Lippard, *Science* **1995**, *268*, 996–997.
[6] P. A. Karplus, M. A. Pearson, R. P. Hausinger, *Acc. Chem. Res.* **1997**, *30*, 330–337.
[7] a) S. Ciurli, XXXIII International Conference on Coordination Chemistry, Florence, Italy, Aug 30–Sept 4, **1998**; S. Benini, W. R. Rypniewski, K. S. Wilson, S. Mangani, S. Ciurli, *J. Biol. Inorg. Chem.* **1998**, *3*, 268–273.
[8] M. W. Göbel, *Angew. Chem.* **1994**, *106*, 1201–1203; *Angew. Chem. Int. Ed. Engl.* **1994**, *33*, 1141.
[9] Urease models: a) R. M. Buchanan, M. S. Mashuta, K. J. Oberhausen, J. F. Richardson, *J. Am. Chem. Soc.* **1989**, *111*, 4497–4498; b) H. E. Wages, K. L. Taft, S. J. Lippard, *Inorg. Chem.* **1993**, *32*, 4985–4987; c) D. Volkmer, A. Hörstmann, K. Griesar, W. Haase, B. Krebs, *Inorg. Chem.* **1996**, *35*, 1132–1135; d) D. Volkmer, B. Hommerich, K. Griesar, W. Haase, B. Krebs, *Inorg. Chem.* **1996**, *35*, 3792–3803; e) K. Yamaguchi, S. Koshino, F. Akagi, M. Suzuki, A. Uehara, S. Suzuki, *J. Am. Chem. Soc.* **1997**, *119*, 5752–5753; f) T. Koga, H. Furutachi, T. Nakamura, N. Fukita, M. Ohba, K. Takahashi, H. Okawa, *Inorg. Chem.* **1998**, *37*, 989–996.
[10] F. Meyer, K. Heinze, B. Nuber, L. Zsolnai, *J. Chem. Soc. Dalton Trans.* **1998**, 207–213.
[11] F. Meyer, P. Rutsch, *Chem. Commun.* **1998**, 1037–1038.
[12] a) E. C. Wilkinson, Y. Dong, L. Que, Jr., *J. Am. Chem. Soc.* **1994**, *116*, 8394–8395; b) A. Hazell, K. B. Jensen, C. J. McKenzie, H. Toftlund, *Inorg. Chem.* **1994**, *33*, 3127–3134; c) C. Duboc-Toia, S. Menage, J.-M. Vincent, M. T. Averbuch-Pouchot, M. Fontecave, *Inorg. Chem.* **1997**, *36*, 6148–6149.
[13] F. Meyer, A. Jacobi, B. Nuber, P. Rutsch, L. Zsolnai, *Inorg. Chem.* **1998**, *37*, 1213–1218.
[14] F. Meyer, H. Pritzkow, *Chem. Commun.* **1998**, 1555–1556.
[15] a) T. Kamiusuki, H. Okawa, E. Kitaura, K. Inoue, S. Kida, *Inorg. Chim. Acta* **1991**, *179*, 139–143; b) M. Itoh, K. Motoda, K. Shindo, T. Kamiusuki, H. Sakiyama, N. Matsumoto, H. Okawa, *J. Chem. Soc. Dalton Trans.* **1995**, 3635–3641; c) F. Meyer, S. Beyreuther, K. Heinze, L. Zsolnai, *Chem. Ber./Recueil* **1997**, *130*, 605–613.
[16] M. Ardon, A. Bino, *Struct. Bonding (Berlin)*, **1987**, *65*, 1–28.
[17] A. W. Addison, T. N. Rao, J. Reedijk, J. van Rijn, G. C. Verschoor, *J. Chem. Soc. Dalton Trans.* **1984**, 1349–1356.
[18] O. Kahn, *Molecular Magnetism*, VCH, New York, **1993**.
[19] C. J. O'Connor, *Progr. Inorg. Chem.* **1982**, *29*, 203–283.
[20] N_α refers to the temperature-independent paramagnetism (100×10^{-6} cm^3 mol^{-1} per nickel(II) ion[18]); all other parameters have their usual meaning. χ_{dim} and χ_{mono} are defined in Equations (2) and (3).

$$\chi_{dim} = (Ng^2\mu_B{}^2/kT)[2\exp(2J/kT)+10\exp(6J/kT)]/[1+3\exp(2J/kT)+5\exp(6J/kT)] \quad (2)$$

$$\chi_{mono} = 2Ng^2\mu_B{}^2/3kT \quad (3)$$

[21] P. Chauduri, H.-J. Küppers, K. Wieghardt, S. Gehring, W. Hasse, B. Nuber, J. Weiss, *J. Chem. Soc. Dalton Trans.* **1988**, 1367–1370.
[22] A. C. Fabretti, W. Malavasi, D. Gatteschi, R. Sessoli, *J. Chem. Soc. Dalton Trans.* **1991**, 2331–2334.
[23] V. M. Crawford, M. W. Richardson, J. R. Wasson, D. J. Hodgson, W. E. Hatfield, *Inorg. Chem.* **1976**, *15*, 2107–2110.
[24] a) K. K. Nanda, L. K. Thompson, J. N. Bridson, K. Nag, *J. Chem. Soc. Chem. Commun.* **1994**, 1337–1338; b) K. K. Nanda, R. Das, L. K. Thompson, K. Venkatsubramanian, P. Paul, K. Nag, *Inorg. Chem.* **1994**, *33*, 1188–1193.
[25] F. Meyer, U. Ruschewitz, P. Schober, B. Antelmann, L. Zsolnai, *J. Chem. Soc. Dalton Trans.* **1998**, 1181–1186.
[26] B. R. Penfold, J. C. B. White, *Acta Crystallogr.* **1959**, *12*, 130–135.
[27] a) N. J. Curtis, K. S. Hagen, A. M. Sargeson, *J. Chem. Soc. Chem. Commun.* **1984**, 1571–1573; b) N. W. Alcock, I. I. Creaser, N. J. Curtis, L. Roecker, A. M. Sargeson, A. C. Willis, *Aus. J. Chem.* **1990**, 643–654.
[28] S. T. Frey, N. N. Murthy, S. T. Weintraub, L. K. Thompson, K. D. Karlin, *Inorg. Chem.* **1997**, *36*, 956–957.
[29] a) C. J. McKenzie, R. Robson, *J. Chem. Soc. Chem. Commun.* **1988**, 112–114; b) B. F. Hoskins, C. J. McKenzie, I. A. S. MacDonald, R. Robson, *J. Chem. Soc. Dalton Trans.* **1996**, 2227–2232.

[30] C. B. Bauer, T. E. Concolino, J. L. Eglin, R. D. Rogers, R. J. Staples, *J. Chem. Soc. Dalton Trans.* **1998**, 2813 – 2817.
[31] F. Meyer, E. Kaifer, unpublished results.
[32] a) D. M. Duggan, D. N. Hendrickson, *Inorg. Chem.* **1974**, *13*, 2056 – 2062; b) A. Escuer, R. Vicente, M. Salah El Fallah, X. Solans, M. Font-Bardia, *J. Chem. Soc. Dalton Trans.* **1996**, 1013 – 1019.
[33] a) W. H. R. Shaw, J. J. Bordeaux, *J. Am. Chem. Soc.* **1955**, *77*, 4729 – 4733; b) R. L. Blakeley, A. Treston, R. K. Andrews, B. Zerner, *J. Am. Chem. Soc.* **1982**, *104*, 612 – 614.
[34] N. J. Curtis, N. E. Dixon, A. M. Sargeson, *J. Am. Chem. Soc.* **1983**, *105*, 5347 – 5353.
[35] a) D. P. Fairlie, W. G. Jackson, G. M. McLaughlin, *Inorg. Chem.* **1989**, *28*, 1983 – 1989; b) A. A. Watson, D. P. Fairlie, *Inorg. Chem.* **1995**, *34*, 3087 – 3092.
[36] a) M. Di Vaira, F. Mani, P. Stoppioni, *J. Chem. Soc. Dalton Trans.* **1994**, 3739 – 3743; b) M. Di Vaira, F. Mani, N. Nardi, P. Stoppioni, A. Vacca, *J. Chem. Soc. Dalton Trans.* **1996**, 2679 – 2684; c) M. Di Vaira, F. Mani, M. Menicatti, P. Stoppioni, A. Vacca, *J. Chem. Soc. Dalton Trans.* **1997**, 661 – 667.
[37] a) V. P. Hanot, T. D. Robert, J. Kolnaar, J. G. Haasnot, J. Reedijk, H. Kooijman, A. L. Spek, *J. Chem. Soc. Dalton Trans.* **1996**, 4275 – 4281; b) R. Deters, R. Krämer, *Inorg. Chim. Acta* **1998**, *269*, 117 – 124.
[38] R. G. Jones, *J. Am. Chem. Soc.* **1949**, *71*, 3994 – 4000.
[39] D. Nicholls, in *Comprehensive Inorganic Chemistry, Vol. 3* (Eds.: J. C. Bailar, H. J. Emeléus, R. Nyholm, A. F. Trotman-Dickenson), 1st ed., Pergamon, Oxford, **1973**, p. 1152 ff.
[40] a) R. Breslow, R. Fairweather, J. Keana, *J. Am. Chem. Soc.* **1967**, *89*, 2135 – 2138; b) J. Chin, J. H. Kim, *Angew. Chem.* **1990**, *102*, 580 – 582; *Angew. Chem. Int. Ed. Engl.* **1990**, *29*, 523; c) J. H. Kim, J. Britten, J. Chin, *J. Am. Chem. Soc.* **1993**, *115*, 3618 – 3622.
[41] M. A. De Rosch, W. C. Trogler, *Inorg. Chem.* **1990**, *29*, 2409 – 2416.
[42] a) E. Kövári, R. Krämer, *Chem. Ber.* **1994**, *127*, 2151 – 2157; b) E. Kövári, R. Krämer, *J. Am. Chem. Soc.* **1996**, *118*, 12704 – 12709.
[43] See for example: a) W. H. Chapman, R. Breslow, *J. Am. Chem. Soc.* **1995**, *117*, 5462 – 5469; b) M. Y. Young, J. Chin, *J. Am. Chem. Soc.* **1995**, *117*, 10577 – 10578; c) M. Yashiro, A. Ishikubo, M. Komiyama, *J. Chem. Soc. Chem. Commun.* **1995**, 1793 – 1794; d) T. Koike, M. Inoue, E. Kimura, M. Shiro, *J. Am. Chem. Soc.* **1996**, *118*, 3091 – 3099; e) C. Wendelstorf, S. Warzeska, E. Kövári, R. Krämer, *J. Chem. Soc. Dalton Trans.* **1996**, 3087 – 3092; f) K. G. Ragmathan, H.-J. Schneider, *Angew. Chem.* **1996**, *108*, 1314 – 1316; *Angew. Chem. Int. Ed. Engl.* **1996**, *35*, 1219 – 1221; g) P. Molenvald, J. F. J. Engbersen, H. Kooijman, A. L. Spek, D. N. Reinhoudt, *J. Am. Chem. Soc.* **1998**, *120*, 6726 – 6737.
[44] G. B. Deacon, R. J. Phillips, *Coord. Chem. Rev.* **1980**, *33*, 227 – 250.
[45] G. M. Sheldrick, *SHELXL-97, Program for Crystal Structure Refinement*, Universität Göttingen, **1997**; *SHELXS-97, Program for Crystal Structure Solution*, Universität Göttingen, **1997**.
[46] L. Zsolnai, G. Huttner, *XPMA*, Universität Heidelberg, **1998**; www.heidelberg.de/~v54/xpm.html.

Received: November 20, 1998 [F1455]

  0947-6539/99/0505-1630 $ 17.50+.50/0